Digital Comprehensive Summaries of Uppsala Dissertations
from the Faculty of Medicine 2224

Affibody Molecule-mediated Radionuclide Therapy of HER2-expressing Cancers

YONGSHENG LIU

ACTA UNIVERSITATIS
UPSALIENSIS
2026

ISSN 1651-6206
ISBN 978-91-513-2704-4
urn:nbn:se:uu:diva-572728

UPPSALA
UNIVERSITET

Dissertation presented at Uppsala University to be publicly examined in Rudbecksalen, Rudbeck laboratory, Dag Hammarskjölds Väg 20, Uppsala, Friday, 6 February 2026 at 09:00 for the degree of Doctor of Philosophy (Faculty of Medicine). The examination will be conducted in English. Faculty examiner: Assistant professor Erik de Blois (Department of Radiology and Nuclear Medicine, Erasmus MC, Rotterdam, The Netherlands).

Abstract

Liu, Y. 2026. Affibody Molecule-mediated Radionuclide Therapy of HER2-expressing Cancers. *Digital Comprehensive Summaries of Uppsala Dissertations from the Faculty of Medicine* 2224. 77 pp. Uppsala: Acta Universitatis Upsaliensis. ISBN 978-91-513-2704-4.

Human Epidermal Growth Factor Receptor 2 (HER2) is over-expressed in several cancers, including breast, gastric, ovarian, and lung cancers. Although HER2-targeted monoclonal antibodies have improved clinical outcomes, resistance remains a major challenge. Their large molecular size also limits tumor penetration and leads to prolonged circulation, increasing off-target toxicity. Affibody molecules offer an attractive alternative due to their small size (~7 kDa), high stability, and strong, specific HER2 binding. Their rapid tumor penetration and fast blood clearance make them suitable for imaging and Targeted Radionuclide Therapy (TRT). Therapeutic radionuclides like lutetium-177 and rhenium-188 can be site specifically labeled with Affibody molecules via conjugated chelators, enabling selective delivery of cytotoxic radiation to HER2-expressing tumors. A major limitation of Affibody-based TRT is high renal uptake. Strategies such as non-residualizing labels and fusion with albumin-binding domains (ABD) aim to improve biodistribution. Non-residualiz-ing labels utilize the slow internalization of HER2-bound Affibody molecules in tumors while allowing rapid renal clearance, resulting in higher tumor-to-kidney ratios. ABD fusion prolongs circulation by binding to serum albumin, reducing renal filtration and enhancing tumor accumulation. These approaches form the basis of the work summarized in this thesis.

Paper I showed that the non-residualizing label, [^{188}Re]Re-$Z_{HER2:41071}$ pro-vided favorable tumor-to-kidney ratios and improved survival in mice without organ toxicity. **Paper II** evaluated chelator positioning in ABD-fused constructs and demonstrated that placing DOTA to helix 1 of ABD did not reduce renal uptake. **Paper III** showed that chemo-enzymatic peptide synthesis enables production of ABD-fused Affibody molecules with preserved structure, HER2 affinity, albumin binding, and in vivo targeting. **Paper IV** demonstrated that [^{177}Lu]Lu-ABY-027, alone or combined with trastuzumab, significantly prolonged survival in xenografted mice, with combination therapy providing better outcome. **Paper V** introduced a variant with deimmunized ABD, PEP49989, which improved biodistribution profile and provided potent therapeutic efficacy, further enhanced by trastuzumab, with minimal renal and hepatic toxicity.

In conclusion, strategies such as non-residualizing label and ABD fusion enable effective tumor targeting and therapeutic effects. These advances validate Affibody-based TRT as a promising complement to existing HER2-directed therapies and provide important design principles for next-generation radio-pharmaceuticals with improved safety, efficacy, and translational potential.

Keywords: Affibody molecule, HER2, targeted radionuclide therapy, tumor targeting, lutetium-177, rhenium-188, non-residualizing label, albumin-bind-ing domain (ABD)

Yongsheng Liu, Department of Immunology, Genetics and Pathology, Cancer precision medicine, Dag Hammarskjölds väg 20, Uppsala University, SE-751 85 Uppsala, Sweden.

ISSN 1651-6206
ISBN 978-91-513-2704-4
URN urn:nbn:se:uu:diva-572728 (http://urn.kb.se/resolve?urn=urn:nbn:se:uu:diva-572728)

To Mia

List of Papers

This thesis is based on the following papers, which are referred to in the text by their Roman numerals.

I. **Liu, Y.**, Vorobyeva, A., Orlova, A., Konijnenberg, M. W., Xu, T., Bragina, O., Loftenius, A., Rosander, E., Frejd, F. Y., Tolmachev, V. (2022) Experimental Therapy of HER2-Expressing Xenografts Using the Second-Generation HER2-Targeting Affibody Molecule ^{188}Re-ZHER2:41071. *Pharmaceutics*, 14(5):1092.

II. **Liu, Y.**, Vorobyeva, A., Xu, T., Orlova, A., Loftenius, A., Bengtsson, T., Jonasson, P., Tolmachev, V., Frejd, F. Y. (2021) Comparative Preclinical Evaluation of HER2-Targeting ABD-Fused Affibody® Molecules ^{177}Lu-ABY-271 and ^{177}Lu-ABY-027: Impact of DOTA Position on ABD Domain. *Pharmaceutics*, 13(6):839.

III. **Liu, Y.**, Güler, R., Liao, Y., Vorobyeva, A., Widmark, O., Meuleman, T. J., Koijen, A., van den Bos, L. J., Naasz, R., Bodenko, V., Orlova, A., Ekblad, C., Tolmachev, V., Frejd, F. Y. (2022) Biologic Evaluation of a Heterodimeric HER2-Albumin Targeted Affibody Molecule Produced by Chemo-Enzymatic Peptide Synthesis. *Pharmaceutics*, 14(11):2519.

IV. **Liu, Y.**, Xu, T., Vorobyeva, A., Loftenius, A., Bodenko, V., Orlova, A., Frejd, F. Y., Tolmachev, V. (2023) Radionuclide Therapy of HER2-Expressing Xenografts Using [^{177}Lu]Lu-ABY-027 Affibody Molecule Alone and in Combination with Trastuzumab. *Cancers*, 15(9):2409.

V. **Liu, Y.**, Oroujeni, M., Liao, Y., Vorobyeva, A., Bodenko, V., Orlova, A., Konijnenberg, M., Carlqvist, M., Wahlberg, E., Loftenius, A., Frejd, F. Y., Tolmachev, V. (2024) Evaluation of a Novel ^{177}Lu-Labelled Therapeutic Affibody Molecule with a Deimmunized ABD Domain and Improved Biodistribution Profile. *European Journal of Nuclear Medicine and Molecular Imaging*, 51(13):4038–4048.

Publications Not Included in This Thesis

I. Tolmachev, V., Vorobyeva, A., Rosly, A. H. B., Garousi, J., **Liu, Y.**, Gräslund, T., Papalanis, E., Schulga, A., Konovalova, E., Orlova, A., Deyev, S. M., Oroujeni, M. (2025) Targeting of Epithelial Cell Adhesion Molecule-Expressing Malignant Tumors Using an Albumin-Binding Domain-Fused Designed Ankyrin Repeat Protein: Effect of the Molecular Architecture. *International Journal of Molecular Sciences*, 26(11):5236.

II. Oroujeni, M., Westerlund, K., Papalanis, E., van Deventer, A., **Liu, Y.**, Clinton, J., Wang, Z., Zelepukin, I., Orlova, A., Tolmachev, V., Eriksson Karlström, A. (2025) Designed Ankyrin Repeat Protein-Mediated Peptide Nucleic Acid-Based Pretargeting: A Proof-of-Principle Study. *Journal of Nuclear Medicine*, 66(7):1105–1111.

III. Lundmark, F., Vorobyeva, A., **Liu, Y.**, Lindbo, S., Xu, T., Oroujeni, M., Rinne, S. S., Rosenström, U., Garousi, J. (2024) Reduction of Renal Activity Retention of Radiolabeled Albumin Binding Domain-Derived Affinity Proteins Using a Non-Residualizing Label Strategy Compared with a Cleavable Glycine-Leucine-Glycine-Lysine-Linker. *Molecular Medicine Reports*, 29(2):32.

IV. Zhang, X., Li, M., Ye, S., Shen, K., Yuan, H., Bakhtyar, S., Peng, Q., **Liu, Y.**, Wang, Y., Li, M., Zhang, C., Wang, Y., Bai, X., Liu, S., Zhao, K., Shen, B., Repsilber, D., Hu, G., Zhang, H., Sun, X. F. (2023) CBD2: A Functional Biomarker Database for Colorectal Cancer. *iMeta*, 3(1):e155.

V. Oroujeni, M., Bezverkhniaia, E. A., Xu, T., **Liu, Y.**, Plotnikov, E. V., Klint, S., Ryer, E., Karlberg, I., Orlova, A., Frejd, F. Y., Tolmachev, V. (2023) Evaluation of Affinity-Matured Affibody Molecules for Imaging of the Immune Checkpoint Protein B7-H3. *Nuclear Medicine and Biology*, 124–125:108384.

VI. Dahlsson Leitao, C., Mestre Borras, A., Xu, T., Oroujeni, M., **Liu, Y.**, Westerberg, C., Clinton, J., Tolmachev, V., Orlova, A., Ståhl, S., Vorobyeva, A., Löfblom, J. (2023) Conditionally Activated Affibody-Based Prodrug Targeting EGFR Demonstrates Improved Tumour Selectivity. *Journal of Controlled Release*, 357:185–195.

VII. Yin, W., Xu, T., Ding, H., Zhang, J., Bodenko, V., Tretyakova, M. S., Belousov, M. V., **Liu, Y.**, Oroujeni, M., Orlova, A., Tolmachev, V., Gräslund, T., Vorobyeva, A. (2023) Comparison of HER2-Targeted Affibody Conjugates Loaded with Auristatin- and Maytansine-Derived Drugs. *Journal of Controlled Release*, 355:515–527.

VIII. Oroujeni, M., Bezverkhniaia, E. A., Xu, T., **Liu, Y.**, Plotnikov, E. V., Karlberg, I., Ryer, E., Orlova, A., Tolmachev, V., Frejd, F. Y. (2022) Evaluation of an Affibody-Based Binder for Imaging of Immune Checkpoint Molecule B7-H3. *Pharmaceutics*, 14(9):1780.

IX. Garousi, J., Xu, T., **Liu, Y.**, Vorontsova, O., Hober, S., Orlova, A., Tolmachev, V., Gräslund, T., Vorobyeva, A. (2022) Experimental HER2-Targeted Therapy Using ADAPT6-ABD-mcDM1 in Mice Bearing SKOV3 Ovarian Cancer Xenografts: Efficacy and Selection of Companion Imaging Counterpart. *Pharmaceutics*, 14(8):1612.

X. **Liu, Y.**, Yu, S., Xu, T., Bodenko, V., Orlova, A., Oroujeni, M., Rinne, S. S., Tolmachev, V., Vorobyeva, A., Gräslund, T. (2022) Preclinical Evaluation of a New Format of ^{68}Ga- and ^{111}In-Labeled Affibody Molecule ZIGF-1R:4551 for the Visualization of IGF-1R Expression in Malignant Tumors Using PET and SPECT. *Pharmaceutics*, 14(7):1475.

XI. Xu, T., **Liu, Y.**, Schulga, A., Konovalova, E., Deyev, S. M., Tolmachev, V., Vorobyeva, A. (2022) Epithelial Cell Adhesion Molecule-Targeting Designed Ankyrin Repeat Protein-Toxin Fusion Ec1-LoPE Exhibits Potent Cytotoxic Action in Prostate Cancer Cells. *Oncology Reports*, 47(5):94.

XII. Oroujeni, M., Tano, H., Vorobyeva, A., **Liu, Y.**, Vorontsova, O., Xu, T., Westerlund, K., Orlova, A., Tolmachev, V., Karlström, A. E. (2022) Affibody-Mediated PNA-Based Pretargeted Cotreatment Improves Survival of Trastuzumab-Treated Mice Bearing HER2-Expressing Xenografts. *Journal of Nuclear Medicine*, 63(7):1046–1051.

XIII. Deyev, S. M., Xu, T., **Liu, Y.**, Schulga, A., Konovalova, E., Garousi, J., Rinne, S. S., Larkina, M., Ding, H., Gräslund, T., Orlova, A., Tolmachev, V., Vorobyeva, A. (2021) Influence of the Position and Composition of Radiometal and Radioiodine Labels on Imaging of EpCAM Expression in a Prostate Cancer Model Using the DARPin Ec1. *Cancers*, 13(14):3589.

XIV. Tano, H., Oroujeni, M., Vorobyeva, A., Westerlund, K., **Liu, Y.**, Xu, T., Vasconcelos, D., Orlova, A., Karlström, A. E., Tolmachev, V. (2021) Comparative Evaluation of Novel ^{177}Lu-Labeled PNA Probes for Affibody-Mediated PNA-Based Pretargeting. *Cancers*, 13(3):500.

XV. Vorobyeva, A., Oroujeni, M., Lindbo, S., Hober, S., Xu, T., **Liu, Y.**, Rinne, S. S., Garousi, J. (2020) Investigation of a Pharmacological Approach for Reduction of Renal Uptake of Radiolabeled ADAPT Scaffold Protein. *Molecules*, 25(19):4448.

Contents

Abbreviations

ABD	Albumin binding domain
ADC	Antibody-drug conjugate
ATCC	American Type Culture Collection
BC	Breast cancer
BTC	Biliary tract cancer
CEPS	Chemo-Enzymatic Peptide Synthesis
CT	Computed tomography
DOTA	1,4,7,10-tetraazacyclododecane-1,4,7,10-tetraacetic acid
DNA	Deoxyribonucleic acid
EDTA	Ethylenediaminetetraacetic acid
EGFR	Epidermal growth factor receptor
EMA	European Medicines Agency
FDA	Food and Drug Administration
GC	Gastric cancer
GEJ	Gastroesophageal junction
HCC	Hepatocellular carcinoma
HEDP	Hydroxyethylidene diphosphonate
HER	Human epidermal growth factor receptor
HER2	Human epidermal growth factor receptor 2
HER3	Human epidermal growth factor receptor 3
HER4	Human epidermal growth factor receptor 4
HSA	Human serum albumin
iTLC	instant thin layer chromatography
i.v.	Intravenous injection
K_D	Dissociation equilibrium constant
LC-MS	Liquid chromatography-mass spectrometry
LET	Linear energy transfer
mAb	Monoclonal antibody
MSA	Mouse serum albumin
NMPA	National Medical Products Administration
NSCLC	Non-small cell lung cancer
PBS	Phosphate-buffered saline
PD-1	Programmed cell death protein 1

PD-L1	Programmed Cell Death Ligand 1
PDGFRβ	Platelet-derived growth factor receptor β
p.i.	Post-injection
PMDA	Pharmaceuticals and Medical Devices Agency
PNA	Peptide nucleic acid
RIT	Radioimmunotherapy
RC48-ADC	Disitamab Vedotin
s.c.	Subcutaneous injection
SPECT	Single-photon emission computed tomography
SPR	Surface Plasmon Resonance
TKI	Tyrosine kinase inhibitor
TRT	Targeted radionuclide therapy
T-DM1	Ado-trastuzumab emtansine
T-DXd	Fam-trastuzumab deruxtecan-nxki
VEGFR2	Vascular endothelial growth factor receptor 2
-GGGC	Glycyl-glycyl-glycyl-cysteinyl
%ID/g	Percent injected dose per gram
%ID	Percent injected dose

Introduction

Chapter I Cancer and Cancer Therapy

Cancer remains one of the most pressing global health challenges. According to the most recent estimates, nearly 20 million new cases and 10 million deaths occurred worldwide in 2020, making cancer the second leading cause of death after cardiovascular diseases [1]. The fundamental problem in cancer therapy lies in the heterogeneity and adaptability of malignant cells. Tumors evolve mechanisms to evade immune surveillance, repair DNA damage, and resist apoptosis, making them difficult to eradicate with conventional treatments [2]. Current therapeutic options include surgery, which is often curative in localized disease; radiotherapy, which uses external beams of ionizing radiation to kill cancer cells; and systemic therapies such as chemotherapy. Each modality has its own advantages and limitations. The main limitations of surgery and radiotherapy are that they are generally applicable to localized tumors. However, when the disease has disseminated and spread to several locations, systemic treatment is required to reach all of them. Chemotherapy, as a part of conventional systemic treatments, often has limited efficacy, as the doses required for cancer eradication are associated with significant toxicity [3, 4].

Over the last two decades, precision medicine approaches have reached the oncology practice. They include therapies that are directed specifically to molecular targets, which are often mutated, amplified or overexpressed proteins present in higher amounts in cancer cells compared to normal cells. Selected examples of targeted therapies include monoclonal antibodies, tyrosine kinase inhibitors, and immune checkpoint inhibitors, all of which have provided remarkable survival benefits for patients [5]. Still, tumors in many patients fail to respond to targeted therapy because cancer cells frequently develop resistance by acquiring additional mutations or by developing alternative signaling pathways. In addition, some patients might not respond due to the absence of specific molecular targets, while some might respond only partially due to heterogeneity of target expression in the tumor [6]. Recent breakthroughs in immunotherapy, such as the development of PD-1 inhibitors, have expanded the range of treatment options and shown anti-tumor responses in patients with different tumor types. However, they still benefit only a fraction of patients [7].

These challenges highlight the need for the development of novel therapies that combine molecular precision with potent cytotoxic effects. Targeted radionuclide therapy (TRT) is one such modality. By coupling a cytotoxic radionuclide with a carrier molecule that is specific to the molecular target expressed on tumor cells, TRT delivers lethal absorbed dose directly to malignant cells while sparing or reducing damage to healthy tissues. Unlike small-molecule inhibitors or antibodies that act by blocking signaling pathways, TRT uses ionizing radiation to induce DNA damage, making cancer cells less prone to developing resistance mechanisms [8]. Furthermore, the ability of some radionuclides to co-emit therapeutic β^-- or α-particles and γ- or positron-emitting photons enables theranostics, an approach that combines therapy with imaging and personalized dosimetry [9].

Chapter II HER2 as a Therapeutic Target

Human epidermal growth factor receptor 2 (HER2, encoded by the ERBB2 gene) is a transmembrane receptor tyrosine kinase belonging to the human epidermal growth factor receptor (HER) family, together with EGFR, HER3, and HER4. HER2 lacks a known natural ligand, but it functions as a preferred dimerization partner for other HER family members. Formation of these dimers leads to potent activation of downstream signaling pathways that regulate cell growth, survival, and proliferation [10]. HER2 is expressed at a low level on normal epithelial cells in gastro-intestinal, respiratory, reproductive, urinary tract, skin and breast [11]. Overexpression or amplification of HER2 occurs in approximately 15-30% of breast cancers, 10-30% of gastric/gastroesophageal cancers, and 20-30% of ovarian cancers [12]. Its amplification is strongly associated with aggressive tumor biology, poor prognosis and reduced overall survival for patients with HER2-positive cancers [13].

The clinical use of HER2 as a therapeutic target was established with the development of trastuzumab in 1998. Trastuzumab is a humanized monoclonal antibody that binds to the extracellular domain IV of HER2, preventing its dimerization and mediating antibody-dependent cellular cytotoxicity [14]. Other HER2-directed therapies have been developed, including pertuzumab, another monoclonal antibody that blocks HER2 dimerization, receptor tyrosine kinase inhibitors (TKI), as well as antibody-drug conjugates (ADCs), with selected examples presented in Table 1.

Table 1. Selected examples of globally approved HER2-targeted therapies.

Name	Trade name	Drug Type	Indication	Approval Agency	Year of first approval
Trastuzumab	Herceptin®	mAb	HER2+ BC; HER2+ GC	FDA (US), EMA (EU), PMDA (Japan), NMPA (China)	1998
Pertuzumab	Perjeta®	mAb	HER2+ BC	FDA, EMA, PMDA	2012
Margetuximab-cmkb	Margenza®	mAb	HER2+ BC	FDA	2020
Zanidatamab	Ziihera®	mAb	HER2+ BTC	FDA; EMA; NMPA	2024
Lapatinib	Tykerb®	TKI	HER2+ BC	FDA, EMA, PMDA	2007
Neratinib	Nerlynx®	TKI	HER2+ BC	FDA, EMA	2017
Tucatinib	Tukysa®	TKI	HER2+ BC	FDA, EMA	2020
Pyrotinib	Irene® / Hengrui®	TKI	HER2+ BC	NMPA	2018
Ado-trastuzumab emtansine (T-DM1)	Kadcyla®	ADC	HER2+ BC	FDA, EMA, PMDA	2013
Fam-trastuzumab deruxtecan-nxki (T-DXd)	Enhertu®	ADC	HER2+ BC; HER2-low BC; HER2-mutant NSCLC; HER2+ GC and GEJ carcinoma	FDA, EMA, PMDA	2019
Disitamab Vedotin (RC48-ADC)	Aidixi® / Vedicitum®	ADC	HER2+ GC and GEJ carcinoma	NMPA	2021

Abbreviations: ADC: antibody-drug conjugate; BC: breast cancer; BTC: biliary tract cancer; EMA: European Medicines Agency; FDA: Food and Drug Administration; GC: gastric cancer; GEJ: gastroesophageal junction; mAb: monoclonal antibody; NMPA: National Medical Products Administration; NSCLC: non-small cell lung cancer; PMDA: Pharmaceuticals and Medical Devices Agency; TKI: tyrosine kinase inhibitor.

However, resistance will develop with application of anti-HER2 therapies through multiple mechanisms, such as downregulation or structural alteration of HER2, activation of alternative signaling pathways, and impaired internalization [15]. It limits the application of conventional HER2-targeted modalities and emphasize the need for alternative strategies to bypass such escape pathways. HER2 is an attractive target for TRT due to the combination of several factors. It is localized on the cell surface, facilitating target recognition and binding of ligands. When overexpressed, it is present on cancer cells in high amount (millions of receptors per cell), enabling efficient delivery of therapeutic radionuclides. Additionally, its limited expression in normal tissues may be mitigated by approaches that saturate HER2 in normal tissues but not in tumors. Altogether, these features support the use of HER2 as target for radionuclide therapy, enabling high tumor uptake and minimizing radiation exposure of normal tissues.

Chapter III Affibody molecules and albumin-binding domain (ABD)

Affibody molecules are a class of engineered scaffold proteins derived from a three-helix bundle structure (Figure 1) containing 58 amino acids, with a molecular weight of approximately 6-7 kDa [16]. By combinatorial randomization of 13 amino acid positions in helices one and two, a library of Affibody molecules was constructed, followed by molecular display and biopanning against desired targets. Affibody molecules binding specifically to various molecular targets, such as HER2, EGFR, HER3, VEGFR2, and PDGFRβ, have been generated, with the dissociation equilibrium constant (K_D) in the pM range, demonstrating high affinities (Table 2) [17].

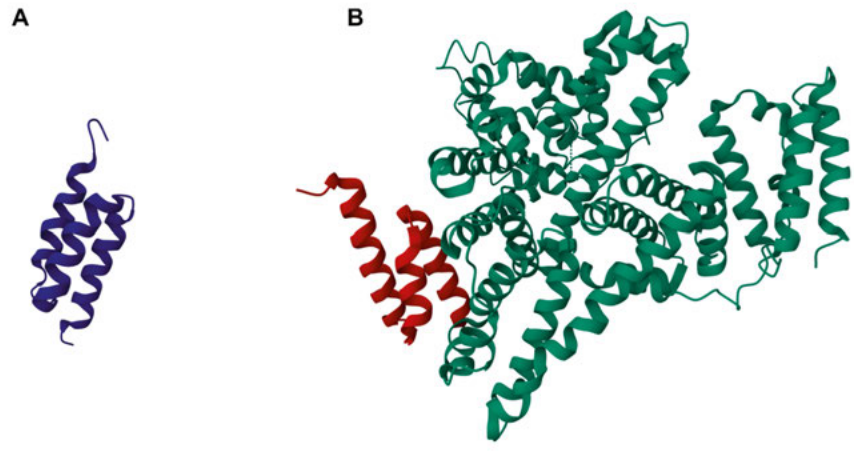

Figure 1. Schematic representation of (A) Affibody molecule Z_{HER2} (PDB: 2KZJ) and (B) ABD (in red) associated to albumin (in green) (PDB: 2VDB). Structures were adjusted from PDB database.

Table 2. Examples of Affibody molecules and affinities to their targets, arranged from highest to lowest affinity.

Molecular target	Affibody variant	K_D
HER2	$Z_{HER2:342}$	22 pM [18]
VEGFR2	Z_{VEGFR2}-Bp_2	30 pM [19]
HER3	$Z_{HER3:08698}$	50 pM [20]
PDGFRβ	$Z_{PDGFRβ:09591}$	92 pM [21]
EGFR	$Z_{EGFR:2377}$	342 pM [22]

Affibody molecules combine small size, high chemical and thermal stability, and straightforward recombinant or peptide synthesis production, which makes them more favorable alternatives to antibodies and antibody fragments for molecular imaging, targeted therapy and theranostic applications [17]. Affibody molecules targeting HER2 were was successfully labeled with ^{111}In and ^{68}Ga, and evaluated in phase I/II clinical trials, showing an excellent visualization of HER2-positive metastases in patients with breast cancer [23, 24]. However, after a fast excretion through the kidneys, Affibody molecules are reabsorbed in the proximal tubuli, which leads to high renal absorbed doses [25]. This is considered as a major limitation for therapeutic applications of Affibody-based radionuclide therapies. The commonly utilized methods for reducing renal uptake of radiolabeled peptides, such as pre- or co-

administration of cationic amino acids or Gelofusine, did not reduce the renal uptake of Affibody molecules [26].

One possible approach to solve this problem is to apply pretargeting, a two-step administration, which separates target recognition and radionuclide delivery [27]. Pretargeting involves administering a target-specific primary agent carrying a recognition tag. Then a radiolabeled secondary agent that interacts with this tag will be injected, once the primary agent has accumulated in tumors and been cleared from non-tumor tissues. HER2-targeted radionuclide therapy using Affibody molecule-based pre-targeting system, $Z_{HER2:342}$-SR-HP1/[^{177}Lu]Lu-HP2, has shown that the renal uptake was 5-fold lower than that in tumor. It also demonstrated significantly increased median survival of mice bearing HER2-expressing xenografts (66 days for the pretargeting group compared to 32 days for [^{177}Lu]Lu-HP2 only) [28]. However, this approach still has its limitations, such as multiple injections, clearance time for the primary agent and regulatory complexity. Therefore, alternative approaches for decreasing renal uptake of radiolabeled Affibody molecules need to be developed.

A characteristic feature of anti-HER2 Affibody molecules is their slow internalization by cancer cells [29]. At the same time, their internalization and catabolism in the kidneys is rapid. This indicates the feasibility of using non-residualizing radiolabels, such as radioiodine, technetium-99m or rhenium-188, for Affibody molecules. The rationale is that the accumulation of radionuclides in tumors relies more on a stable binding of a radiolabeled Affibody molecule to its target on the cellular membrane than on the retention of radiocatabolites within the cells. In the kidneys, Affibody molecules undergo rapid internalization, resulting in rapid release of a non-residualizing label from them. As a result, a few hours after injection of an Affibody molecule carrying a non-residualizing label, its tumor uptake significantly surpasses the uptake in the kidneys, thereby holding the potential for radionuclide therapy [30, 31].

Another effective strategy to overcome high kidney uptake is fusion of Affibody molecules with albumin-binding domain (ABD) for prevention of their glomerular filtration and extension of half-life in blood circulation. ABD is a three-helix motif consisting of 46 amino acids and binds reversibly to serum albumin (Figure 1) with high affinity [32]. Human serum albumin (HSA), with a molecular weight of 66.5 kDa, is the most abundant protein in blood circulation (50-60% of total plasma protein, 35-50 g/L in humans), with an average half-life of three weeks [33]. The binding of ABD-fused Affibody molecules to albumin leads to the formation of a large complex with a molecular weight of around 80 kDa, which is above the kidney filtration barrier of 60 kDa. In this case, blood retention of Affibody molecules is enhanced, leading to

increased accumulation in tumor and increase of the absorbed dose to tumor [17]. This strategy was first demonstrated in 2007 by Tolmachev et al. using dimerized first generation Affibody molecule $Z_{HER2:342}$, labeled with lutetium-177. This construct resuled in significantly increased blood retention and reduced kidney uptake [34]. The conjugate containing the second generation Affibody molecule $Z_{HER2:2891}$ and ABD_{035} has demonstrated improved biodistribution to deliver lutetium-177 [35] or cytotoxic drug DM1 to tumor xenografts in mice [36]. The efficacy and safety of using ABD to extend the blood circulation of Affibody molecules has been demonstrated in clinical trials. Affibody molecule izokibep targeting interleukin-17A showed good tolerance and efficacious treatment in patients in phase II studies [37, 38].

Building on these findings, the current thesis investigates two strategies to reduce kidney uptake during targeted radionuclide therapy using Affibody molecules targeting human HER2. In Paper I, we investigated the use of a non-residualizing rhenium-188 label, and in Papers II-V, we applied modification of pharmacokinetics by fusing Affibody molecules to ABD, and studied their biodistribution, tumor-targeting properties, and anti-tumor effects in vivo. The abbreviated structures of Affibody molecules and their conjugates used in Papers I-V are presented in Table 3.

Table 3. Designation and abbreviated structures of Affibody molecules used in Papers I-V.

Designation	Abbreviated structure	Radionuclide	Paper
$Z_{HER2:41071}$	$Z_{HER2:41071}$-GGGC	Re-188	Paper I
ABY-027	$Z_{HER2:2891}$-ABD-DOTA	Lu-177	Paper II, Paper IV
ABY-271 (PEP41121)	$Z_{HER2:2891}$-ABD(-DOTA) residual 76[1]	Lu-177	Paper II
PEP40233	DOTA-$Z_{HER2:2891}$-ABD	Lu-177	Paper III
PEP49989	$Z_{HER2:2891}$-ABD*-DOTA[2]	Lu-177	Paper V

[1]For ABY-271, a unique cysteine was introduced in position 76 of the $Z_{HER2:2891}$-ABD fusion corresponding to the cysteine 14 position of the ABD molecule, and DOTA chelator was conjugated to this cysteine. [2]For PEP49989, ABD* denotes a deimmunized variant of ABD.

Chapter IV Radionuclide therapy using rhenium-188 (^{188}Re) and lutetium-177 (^{177}Lu)

TRT is an emerging therapeutic modality that combines the high specificity of molecular targeting with the cytotoxicity of ionizing radiation from radionuclides. The effectiveness of TRT depends not only on the molecular design of the targeting agent and its pharmacokinetics, but also on the physical and chemical properties of the radionuclides [39]. When selecting a radionuclide for TRT, it is important to consider types of decay, energy of emitted particles, physical half-life, and suitable chelators for stable radiolabeling, as well as their conjugation to the targeting molecules. Biological factors related to absorbed doses to tumor compared to normal organs and tissues, radiosensitivity, and response to radiation define the therapeutic outcome of TRT in vivo [40].

Alpha-, beta-particles and Auger electrons emitted from different radionuclides can be used to irradiate tumor cells in TRT [41]. Auger electrons have medium linear energy transfer (LET) (4-26 keV/μm) but the short path length (2-40 μm) limits their efficacy to single cells, and usually requires delivery of radionuclides in close proximity to the nucleus. Alpha-particles have a longer path length (50-100 μm) than Auger electrons and higher LET (80 keV/μm), making them suitable for the treatment of micro-metastases. Beta-particles have lower LET (~0.2 keV/μm) than alpha particles and Auger electrons, they are used for the treatment of medium to large tumors and metastases, depending on their pathlength (up to 12 mm). The physical half-life of the radionuclide also needs to be considered when developing radiopharmaceuticals for TRT, since it has to be matched with the biological half-life of the targeting molecule. The properties of radionuclides for use in TRT are presented in Table 4.

Table 4. Selected examples of radionuclides for TRT (adapted from Stokke C et al. [42] and MIRDspec isotope database).

Radionuclide	Half-life	Decay mode	Maximum particle energy	Average particle energy	Max range in tissue	Photon radiation, keV
^{67}Cu	2.58 d	β^-	561 keV	136 keV	2.0 mm	185 (44%)
^{90}Y	2.67 d	β^-	2.28 MeV	932 keV	10.8 mm	-
^{131}I	8.02 d	β^-	810 keV	182 keV	3.3 mm	364 (82%)
^{161}Tb	6.91 d	β^-, Auger	593 keV (β^-) 3-50 keV (Auger)	154 keV (β^-)	2.1 mm (β^-) 0.5 µm (Auger)	49 (17%), 75 (10%)
^{177}Lu	6.65 d	β^-	498 keV	134 keV	1.7 mm	208 (11%)
^{188}Re	16.9 h	β^-	2.12 MeV	762.6 keV	10.1 mm	155 (15%)
^{211}At	7.21 h	α	-	2.5 MeV	<100 µm (α)	78 (33%)
^{223}Ra	11.43 d	α		5.8 MeV	<100 µm (α)	141 keV
^{225}Ac	9.92 d	α	-	5.9 MeV	<100 µm (α)	218 keV[1] (11.44%)
^{227}Th	18.68 d	α	-	6.0 MeV	<100 µm (α)	236 keV (12.9%)

[1]photon emitted by its daughter francium-221.

Among the clinically relevant and commercially available therapeutic radionuclides, rhenium-188 (^{188}Re) and lutetium-177 (^{177}Lu) were selected for studies in this thesis. ^{188}Re is a high-energy β^- emitter ($E_{\beta(max)}$ = 2.12 MeV) with a relatively short physical half-life of 16.9 hours, making it suitable for the treatment of small to medium-sized tumors. During its decay, gamma rays are also released with an energy of 155 keV, enabling SPECT imaging for dosimetry purposes. Importantly, ^{188}Re can be conveniently obtained from an inexpensive and long-lived tungsten-188/ rhenium-188 generator. Rhenium-188 has similar radiochemistry to technetium-99m, which allows the use of well-established chelators for stable attachment to targeting molecules. Clinically, rhenium-188 has been used with hydroxyethylidene diphosphonate (HEDP) for bone pain palliation in patients suffering from metastases due to breast and prostate cancer [43]. ^{188}Re-labeled antibodies were evaluated in clinical trials for radioimmunotherapy (RIT) in the treatment of leukemia [44] and metastatic melanoma [45]. ^{188}Re-Lipiodol has been investigated in clinical studies for the therapy of hepatocellular carcinoma [46].

Lutetium-177 emits medium-energy β^- particles ($E_{\beta(max)}$ = 497 keV) and has a relatively long half-life of 6.7 days, making it highly suitable for the

treatment of small metastatic lesions or disseminated tumors. It also emits low-energy γ quanta (113 keV and 208 keV), permitting SPECT imaging and monitoring during therapy. The versatile 1,4,7,10-tetraazacyclododecane-1,4,7,10-tetraacetic acid (DOTA) chelator makes radiolabelling with lutetium-177 straightforward and stable, enabling the development of a wide range of peptide- and protein-based radiopharmaceuticals. Clinically, two radiopharmaceuticals with lutetium-177 were approved by the FDA and EMA and successfully applied for radionuclide therapies, such as ^{177}Lu-DOTATATE (Lutathera®) for neuroendocrine tumors [47] and ^{177}Lu-PSMA-617 (Pluvicto®) for metastatic prostate cancer [48], both of which have demonstrated significant survival benefits.

From the biological perspective, the main mechanism of action behind TRT is causing DNA damage. Once the radionuclide-labeled targeting agent binds to its specific molecular target on cancer cells, the emitted ionizing radiation reaches the cell nucleus and deposits energy. This causes double-strand breaks and clustered DNA lesions, which are often difficult to repair and often lead to apoptosis or necrosis [49]. In addition, β- or α-particles emitted from a decaying radionuclide in one cell can travel short distances and irradiate neighboring tumor cells, so called cross-fire effect, which enables effective irradiation even in heterogeneous tumors [42]. This is particularly beneficial for bulky or poorly vascularized lesions. Furthermore, unlike chemotherapy, TRT has a minimal potential to cause resistance. This is because its cytotoxicity comes from physical energy deposition rather than biochemical effect with specific cellular pathways [50]. These biological advantages make TRT a powerful therapeutic approach, achieving both targeted precision and effective cancer cell eradication within the tumor microenvironment.

The physical and biological properties of radiolabeled targeting molecules allow for optimization of the treatment time window and radiation dose distribution according to their biological kinetics. To make radionuclide therapy effective in vivo, several critical parameters must be evaluated before clinical application. The desired characteristics for the therapy to be effective include high tumor uptake and retention, rapid clearance from non-target tissues, and favorable tumor-to-organ ratios. These properties need to be studied through preclinical and clinical pharmacokinetic and biodistribution studies [40]. Comprehensive dosimetry evaluation is essential to estimate the absorbed doses delivered to both tumors and normal organs. Dosimetry could help to not only predict therapeutic efficacy but also ensure the safety of patients by identifying dose-limiting organs [51]. The primary dose-limiting organs in TRT are the bone marrow, kidneys, and liver, due to their high radiosensitivity and involvement in metabolism and excretion of radiopharmaceuticals.

Selection of the optimal treatment regimen depends on dosimetry calculations. Fractionated or multiple-cycle regimens are commonly applied to maximize tumor dose delivery while allowing normal tissue repair between cycles. The number and frequency of treatment cycles are determined based on patient-specific dosimetry, tumor response, and cumulative toxicity limits to achieve maximal therapeutic effect with minimal side effects [52].

For Affibody-based therapeutics, both ^{188}Re and ^{177}Lu are attractive choices. Importantly, Affibody molecules are chemically robust and free from cysteines. This allows introduction of a cysteine at a defined position for a site-specific conjugation with different chelators for labeling with therapeutic radionuclides. Affibody molecules generally have a stable molecular structure and predictable refolding after heating, which enables labelling in harsh conditions, such as high temperature or pH far from physiological pH. Together, the combination of these advantages of Affibody molecules and therapeutic effect of radionuclides, ^{188}Re and ^{177}Lu, provides a powerful platform for developing next-generation agents for TRT.

Aim of This Thesis

The aim of this thesis was to develop and optimize HER2-targeting Affibody molecules for radionuclide therapy of cancer, to have a potent antitumor effect and minimal uptake in normal organs and tissues, especially in the kidneys. For this purpose, several approaches for molecular design were applied to select the most promising variant for further clinical translation.

As high renal reabsorption represents the main limitation for Affibody molecule-based radionuclide therapy, two approaches were evaluated to overcome this problem. The first approach was investigated using a non-residualizing rhenium-188 label to promote rapid clearance of radioactivity from the kidneys (**Paper I**). The second approach was to investigate fusion of Affibody molecules with ABD for extension of their circulation in blood and reduce renal uptake (**Papers II-V**).

Methodology

Production of Affibody molecules

Affibody molecules were produced and characterized by the biotechnological company Affibody AB (Solna, Sweden). The authenticity of Affibody molecules was confirmed by mass spectrometry, and purity was confirmed using liquid chromatography-mass spectrometry (LC-MS).

Radiolabeling with Re-188 and Lu-177

Radiolabeling approach enabled characterization and quantification of functional properties of Affibody molecules both in vitro and in vivo. For labeling with Re-188, a cysteine-containing peptide-based chelator, -GGGC, was positioned at the C-terminus of Affibody molecules. For labeling with Lu-177, Affibody molecules were coupled to a macrocyclic chelator DOTA (Figure 2). Both methods enable site-specific labeling and have earlier been applied to Affibody molecule-based radiopharmaceuticals that demonstrated excellent binding properties and a favorable biodistribution profile [35, 53].

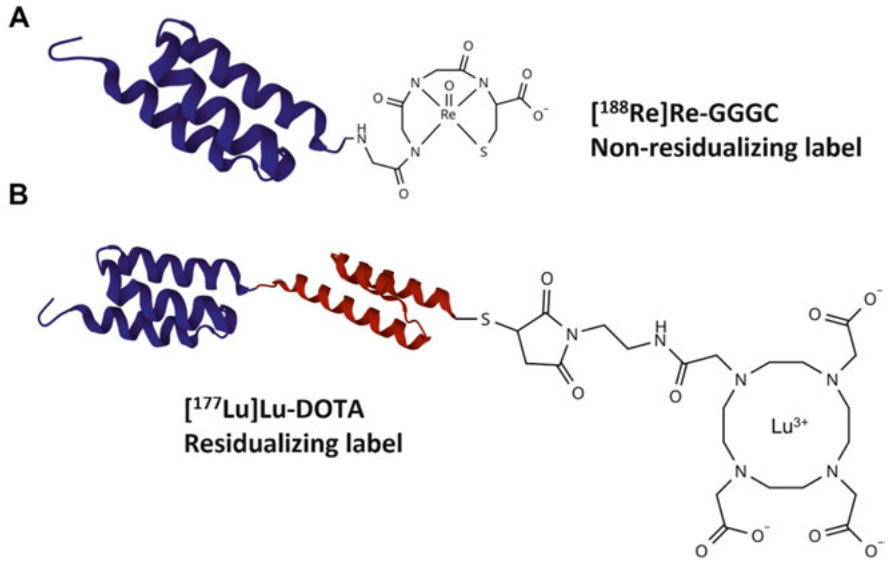

Figure 2. Schematic structure of [^{188}Re]Re-$Z_{HER2:41071}$-GGGC carrying a non-residualizing label and [^{177}Lu]Lu-$Z_{HER2:2891}$-ABD-DOTA carrying a residualizing label.

For labeling of Affibody molecule $Z_{HER2:41071}$ with Re-188 in **Paper I**, a freeze-dried kit containing 1 mg of tin(II) chloride dihydrate, 5 mg of gluconic acid sodium salt and 100 µg of $EDTANa_4$, was dissolved in 1.25 M sodium acetate, pH 4.2, and added to 100 µg of $Z_{HER2:41071}$. The mixture was incubated with ^{188}Re-containing generator eluate at 70 °C for 60 min. The purification was performed using either a size-exclusion NAP-5 column, or an Oasis HLB 1 cc Vac Cartridge, depending on the volume of added eluate. For labelling of ABD-fused Affibody molecules with Lu-177 (in **Papers II to V)**, they were incubated with $^{177}LuCl_3$ in acetate buffer at 65 °C for 30 min. The labeled conjugates were purified using NAP-5 columns, if needed. Radiochemical yield and purity were analyzed using instant thin layer chromatography (iTLC). The stability of the labeled compounds was evaluated by incubation with 500-fold molar excess of ethylenediaminetetraacetic acid (EDTA) or phosphate-buffered saline (PBS) at 37 °C for 60 min.

Cell lines

Cancer cell lines (Table 5) used for in vitro and in vivo assays were obtained from American Type Culture Collection (ATCC) and cultured according to its recommendations.

Table 5. Cell lines used in the studies.

Cell line	HER2 status	HER2 receptors per cell
SKOV3	Over-expressing	1.6×10^6 [54]
BT474	Over-expressing	0.7×10^6 [55]
SKBR3	Over-expressing	1.0×10^6 [55]
BxPC3	Low/intermediate	1.1×10^4 [56]
MDA-MB-468	Negative	1.2×10^3 [57]
Ramos	Negative	-

Note: the number of receptors per cell showed above were saturation assay for SKOV3, BT474, and SKBR3; quantitative immune-fluorescence indirect assay for BxPC3; and FACS analysis for MDA-MB-468.

In vitro studies

The binding specificity assay was performed to evaluate if the binding of Affibody molecules to cells is saturable and HER2-mediated. In the experiment, cells in the blocking group were pre-incubated with a 500-fold molar excess of unlabeled Affibody molecules to saturate HER2 receptors. Thereafter, all cells were incubated with radiolabeled compounds. After incubation, the cells were washed and detached using trypsin-ethylenediaminetetraacetic acid (EDTA) solution (0.25% trypsin, 0.02% EDTA). The percentage of cell-associated activity in blocking and non-blocking groups was calculated and compared.

The binding affinity of Affibody molecules to HER2, HSA, and mouse serum albumin (MSA) was measured by our collaborators at Affibody AB using Surface Plasmon Resonance (Biacore 8K, Cytiva, Uppsala, Sweden).

The affinity of radiolabeled Affibody molecules to living HER2-expressing cells was measured using LigandTracer instruments (Ridgeview Instruments AB, Uppsala, Sweden). Cells were cultured on one side of an 89 mm Petri dish. The other side served as a reference area without cells. A radio-labeled ligand was then added to the dish. The LigandTracer instrument rotated to alternately measure signal from the cell area and the reference area. As the ligand bound to receptors on the cells, the signal intensity increased. The instrument recorded this change continuously, capturing the association phase.

After a period, the ligand solution was replaced with complete media to initiate the dissociation phase. The signal decreased as the ligand unbound from the receptors. The resulting binding curve (signal vs. time) was analyzed to extract kinetic parameters: Association rate constant (ka): how quickly the ligand binds. Dissociation rate constant (kd): how quickly it unbinds. Affinity (K_D): calculated as kd/ka, indicating binding strength.

Cellular processing and internalization assay was performed in the presence of HSA using a modified acid wash method [29]. Cells were incubated with radiolabelled compounds at 37 °C. At pre-determined time points (usually 1, 2, 4, 8 and 24 h), cells were washed and then treated with 0.2 M glycine buffer containing 4 M urea, pH 2.0, for 5 min on ice. The glycine buffer was then collected and the activity was measured and considered as membrane-bound activity. Thereafter, cells were incubated with 1 mL of 1 M NaOH at 37 °C for 20 min and collected. The measured activity was considered as an internalized activity.

Ethical permits

The animal experiments were planned in agreement with EU Directive 2010/63/EU for animal experiments and Swedish national legislation concerning the protection of laboratory animals, and the studies were approved by the local Ethics Committee for Animal Research in Uppsala, Sweden. The permits were: permit C4/16, 26 February 2016 (**Paper II**), and permit 5.8.18-11931/2020, 28 August 2020 (**Paper I, III, IV and V**).

In vivo biodistribution

To investigate the biodistribution and targeting properties of radiolabelled Affibody molecules targeting HER2, biodistribution studies were performed in female BALB/C nu/nu mice bearing SKOV3 xenografts. To establish xenografts, 10^7 SKOV3 cells were injected subcutaneously on the hind leg of mice. The experiments were performed about 3 weeks after implantation. In all biodistribution experiments, typically 4 mice per group were used. HER2-low or -negative xenografts were established by injection of BxPC3 (**Paper III**), or Ramos (**Paper I, II and V)** cells in order to investigate if the binding of radiolabelled Affibody molecules to xenografts was HER2-expression dependent in vivo. As shown in Table 6, mice were injected intravenously with radiolabeled Affibody molecules. At pre-determined time points, mice were euthanized by an intraperitoneal injection of anaesthesia. Blood, tumors, and

tissues/organs of interest were excised, weighed and their activity was measured by an automatic gamma spectrometer (Wizard, Perkin Elmer). The tissue uptake values were calculated as the percentage of injected dose per gram of the sample (%ID/g), while the stomach, intestines, and carcass uptake, were calculated as the percentage of injected dose (%ID) per whole sample.

Table 6. Summary of injected compounds, protein mass, activity used in biodistribution studies.

Paper	Construct	Mw (kDa)	Protein mass per mouse	Injected activity per mouse	Dissection time points p.i.
I	[^{188}Re]Re-$Z_{HER2:41071}$	6.7	10 µg	270 kBq	1, 4, 8, 24, 48 h
II	[^{177}Lu]Lu-ABY-271	12.5	10 µg	260 kBq	4, 24, 48, 72, 168, 336 h
	[^{177}Lu]Lu-ABY-027	12.6	10 µg	260 kBq	48, 168 h
	[^{177}Lu]Lu-ABY-025	7.6	5 µg	260 kBq	48 h
III	[^{177}Lu]Lu-PEP40233	12.5	10 µg	270 kBq	48 h
	[^{177}Lu]Lu-ABY-025	7.6	5 µg	260 kBq	48 h
IV	[^{177}Lu]Lu-ABY-027	12.6	10 µg	270 kBq	48 h
V	[^{177}Lu]Lu-PEP49989	12.5	10 µg	270 kBq	4, 24, 48, 72, 168, 336 h

Therapy studies

In Papers **I, IV and V**, experimental therapy studies were performed using female BALB/C nu/nu mice bearing SKOV3 xenografts to evaluated the therapeutic efficacy and efficiency of radiolabelled Affibody molecules targeting HER2. Mice were subcutaneously implanted on the abdomen with 10^7 SKOV3 cells. The treatment started one week after implantation. Throughout the experiments, tumor volumes and body weights were measured twice per week. The largest longitudinal (length) and transverse (width) diameter were measured by the calliper, and the tumor volume (V) was calculated by the formula: $V = 1/2 \times (\text{length} \times \text{width}^2)$. Mice were euthanized if any of the following humane endpoints were reached: when the tumor volume exceeded 1000 mm^3; when bleeding ulcerations were observed; when overall weight loss was over 15% or when the weight loss was more than 10% within one week. According to the ethical permit, the study was terminated, and all mice were euthanized 90 days after the first injection. To analyse data,

survival curve was plotted by Prisma GraphPad and difference was compared by Log-rank (Mantel-Cox) test. The difference of therapy outcomes was determined using χ^2-test. When mice were euthanized, kidneys and livers were collected, fixed with formalin, and stored in 70% ethanol at 4 °C. The pathology examination was performed by an experienced animal pathologist to evaluate histopathological changes in those organs. The detailed information of experimental therapy studies is summarized in Table 7 and the schematic illustration of therapy studies in Paper IV and V are shown in Figure 3 and 4.

Table 7. Summary of treatment groups, injected compounds, protein mass, activity injection route and frequency in therapy studies.

Paper	Treatment groups	Protein mass per mouse each time	Injected activity per mouse each time	Injected volume	Injection route	Dosing frequency
I	[^{188}Re]Re-$Z_{HER2:41071}$	5 µg	16 MBq	150 µL	i.v.	Three injections with two-day intervals
	Non-labeled $Z_{HER2:41071}$ control	5 µg				
	Vehicle control					
IV	Vehicle control			100 µL	i.v. for the 1st week, and then s.c. weekly for 5 consecutive weeks	
	Non-labeled ABY-027 control	20 µg			i.v. for the 1st week, then s.c. weekly with vehicle for 5 consecutive weeks.	
	[^{177}Lu]Lu-ABY-027	20 µg	20 MBq		i.v. for the 1st week, then s.c. weekly with vehicle for 5 consecutive weeks.	
	Trastuzumab	4 mg/kg and 2 mg/kg			s.c.	4 mg/kg for the 1st week and then with 2 mg/kg for 5 consecutive weeks
	[^{177}Lu]Lu-ABY-027 + trastuzumab	20 µg + 4 mg/kg and 2 mg/kg	20 MBq		i.v. with [^{177}Lu]Lu-ABY-027 and s.c. of trastuzumab 4 mg/kg for the 1st week, then s.c. weekly with 2 mg/kg of trastuzumab for 5 consecutive weeks.	

V	Vehicle control			100 µL	i.v. for the 1st week, and then s.c. weekly for 5 consecutive weeks	
	Trastuzumab	4 mg/kg and 2 mg/kg			s.c.	4 mg/kg for the 1st week and then with 2 mg/kg for 5 consecutive weeks
	[^{177}Lu]Lu-PEP49989 single	10 µg	21 MBq		i.v. for the 1st week, then s.c. weekly with vehicle for 5 consecutive weeks.	
	[^{177}Lu]Lu-PEP49989 double	10 µg	21 MBq		i.v. on day 1 and day 29, and s.c. with vehicle as other groups	
	[^{177}Lu]Lu-PEP49989 + trastuzumab	10 µg + 4 mg/kg and 2 mg/kg	21 MBq		i.v. with [^{177}Lu]Lu-PEP49989 and s.c. of trastuzumab 4 mg/kg for the 1st week, then s.c. weekly with 2 mg/kg of trastuzumab for 5 consecutive weeks.	

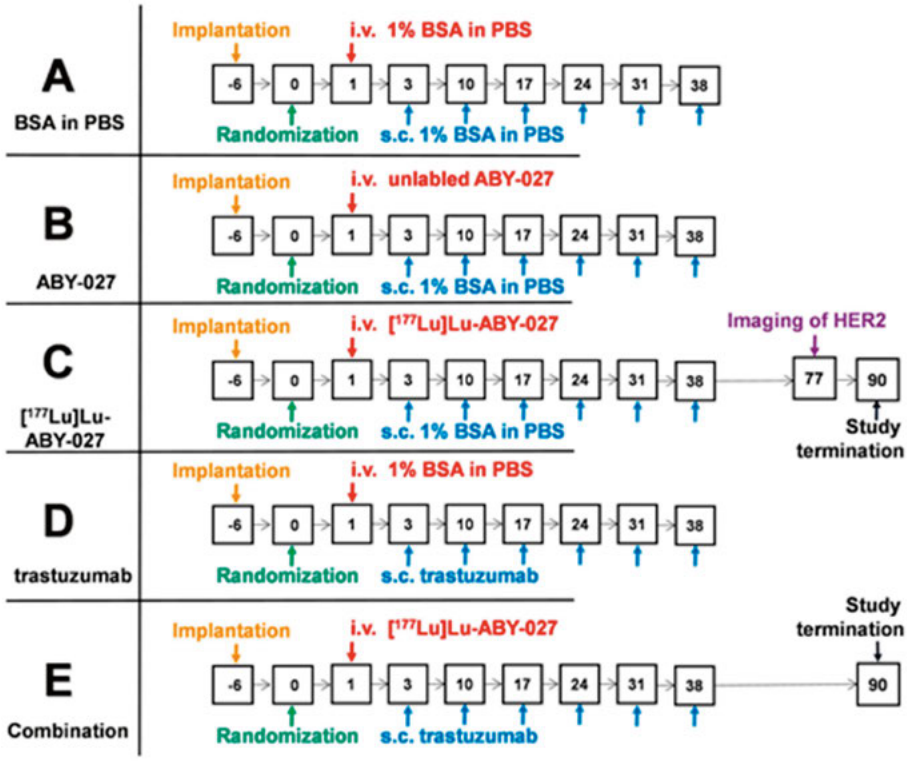

Figure 3. Schematic illustration of the timing of the interventions in therapy experiment in Paper IV.

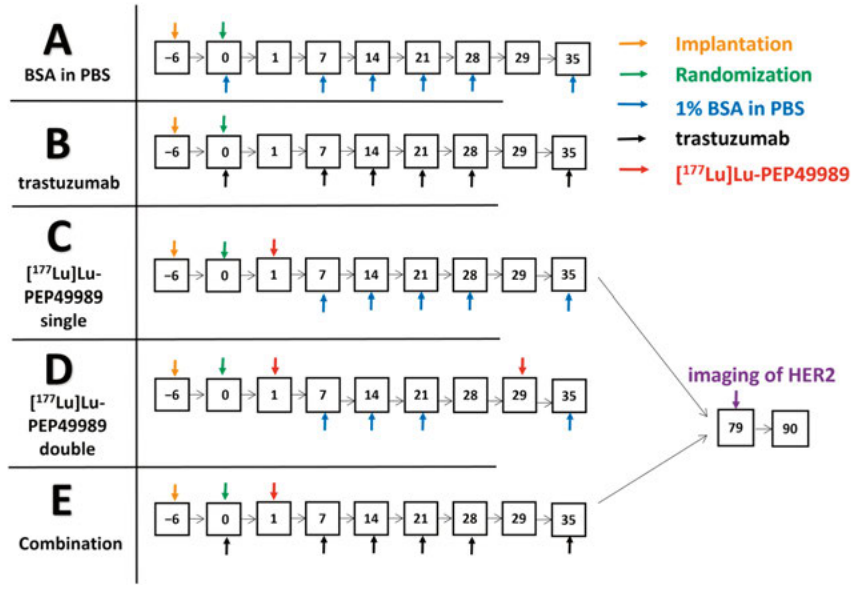

Figure 4. Schematic illustration of the timing of the interventions in therapy experiment in Paper V.

The Present Investigation

Paper I Experimental Therapy of HER2-Expressing Xenografts Using the Second-Generation HER2-Targeting Affibody Molecule ^{188}Re-ZHER2:41071

Background and Aim

Earlier studies have demonstrated that radiolabeled Affibody molecules with non-residualizing properties have stronger retention in tumors than in kidneys. Rinne et al. showed that radioiodine-labelled Affibody, which is a typical non-residualizing label, provided higher tumor-to-kidney ratio and maintaining efficient tumor retention compared with residualizing radiometal labels [58]. Surprisingly, some ^{99m}Tc-based labels also have non-residualizing property. For example, Wållberg et al. previously demonstrated that ^{99m}Tc-labeled anti-HER2 Affibody molecule containing C-terminal -GGGC chelator, designated as ZHER2:V2, has higher accumulation in tumors than renal uptake [59]. The second-generation anti-HER2 Affibody molecule, ^{99m}Tc-$Z_{HER2:41071}$, with -GGGC chelator at C-terminus, which has better thermal and chemical stability and enhanced hydrophilicity, showed the same low renal retention of activity as the ^{99m}Tc-ZHER2:V2 [31]. Rhenium is a chemical analogue of technetium and rhenium-188 emits beta-particles with high energy ($E_{\beta max}$ = 2.1 MeV, $T_{1/2}$ = 17 h), which makes it suitable for radionuclide therapy. Since ^{99m}Tc and ^{188}Re are chemically similar, the chelators used for ^{99m}Tc labeling might also be used for ^{188}Re labeling and provide similar biodistribution properties [60].

Our hypothesis was that ^{188}Re-labeled second-generation anti-HER2 Affibody molecule, $Z_{HER2:41071}$, would have similar properties of binding and biodistribution as ZHER2:V2, and it would be a potential therapeutic agent for the treatment of HER2-expressing malignant tumors. To test the hypothesis, $Z_{HER2:41071}$ was labeled with rhenium-188, and in vitro characterization was performed in HER2-expressing SKOV3 and SKBR3 cell lines. In vivo biodistribution and therapeutic effect of [^{188}Re]Re-$Z_{HER2:41071}$ was studied in Balb/c nu/nu mice bearing SKOV3 xenografts. SPECT/CT imaging of HER2 expression in mice from therapy and control groups was performed using [^{99m}Tc]Tc-$Z_{HER2:41071}$ at day 35.

Results

Labeling of $Z_{HER2:41071}$ with rhenium-188 provided a radiochemical yield of more than 98% (n=8). Purification using an Oasis HLB Cartridge provided the radiochemical purity of 99 ± 1%. In vitro studies confirmed that [^{188}Re]Re-$Z_{HER2:41071}$ specifically bound to HER2-expressing cells, with high affinity (dissociation constant at equilibrium (K_D) was 5 ± 3 pM). Cellular processing profile showed that the cellular uptake and retention of [^{188}Re]Re-ZHER2:2395, which has a residualizing label, was higher at the late time point than [^{188}Re]Re-$Z_{HER2:41071}$ with a non-residualizing label. Slow internalization was observed for both variants in SKOV3 and SKBR3 cells, with less than 15% at 24 h (Figure 5).

Data concerning the biodistribution of [^{188}Re]Re-$Z_{HER2:41071}$ showed a rapid clearance from blood and normal organs, including kidneys. Tumor uptake was 31 ± 4 %ID/g at 1 h after injection, already higher than the uptake in the majority of organs and similar to renal uptake. In the later time points, tumor uptake remained high while accumulation in the kidneys reduced rapidly. Starting from 4 h p.i., uptake in the tumor was more than 8-fold higher than in kidneys (Figure 6). Dosimetry calculation based on biodistribution data showed the absorbed dose to tumor was 3-fold higher than to the kidneys and suggested an injected activity of 16 MBq per therapy cycle for 3 cycles.

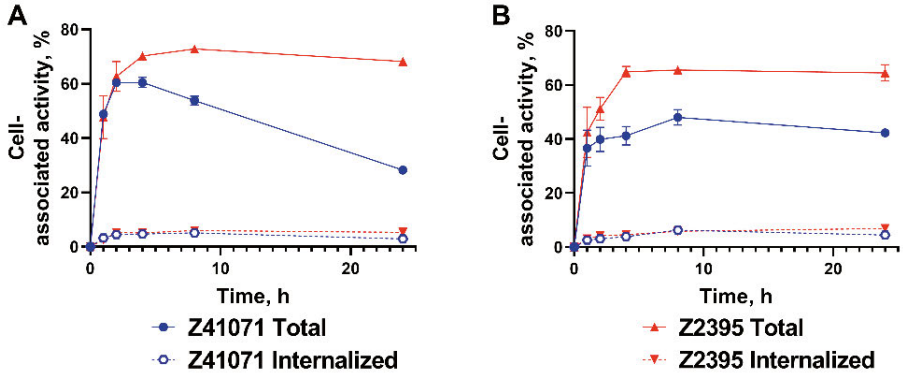

Figure 5. Binding and cellular processing of ^{188}Re-labeled $Z_{HER2:41071}$ and ZHER2:2395 by HER2-expressing SKOV3 (**A**) and SKBR3 (**B**) cells. Data are presented as an average (n = 3) value ± standard deviation (SD).

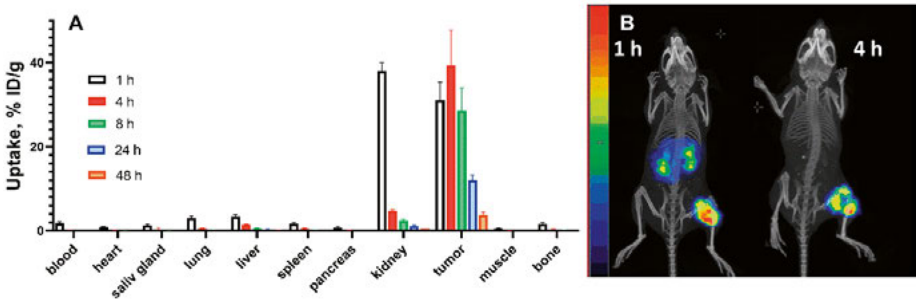

Figure 6. (**A**) Biodistribution of [^{188}Re]Re-$Z_{HER2:41071}$ in Balb/c nu/nu mice bearing HER2-expressing SKOV3 xenografts. Data are presented as an average (n = 4) value ± SD. (**B**) Imaging of Balb/c nu/nu mice bearing HER2-positive SKOV3 xenografts using [^{188}Re]Re-$Z_{HER2:41071}$ at 1 and 4 h after injection. The scale is linear, showing arbitrary units normalized to a maximum count rate.

Experimental therapy study using [^{188}Re]Re-$Z_{HER2:41071}$ showed a reduction of tumor volume starting from day 19 after the first injection. At this time point, the mean tumor volume in the treatment group was significantly smaller ($p < 0.05$) than that in two control groups (one treated with vehicle, another with non-labeled $Z_{HER2:41071}$) (Figure 7). Treatment with [^{188}Re]Re-$Z_{HER2:41071}$ extended median survival to 68 days, which was significantly longer ($p < 0.0001$) than that in control groups (29 days for the vehicle group, 27.5 days for the non-labeled Affibody group) (Figure 8). There was no significant difference in the average animal body weight between the treatment group and the control group. The pathology examination suggested no liver and kidney toxicity of the treatment regimes. SPECT/CT imaging of mice using [^{99m}Tc]Tc-$Z_{HER2:41071}$ enabled visualization of HER2 expression during treatment, and was correlated with the outcome of the therapy (Figure 9).

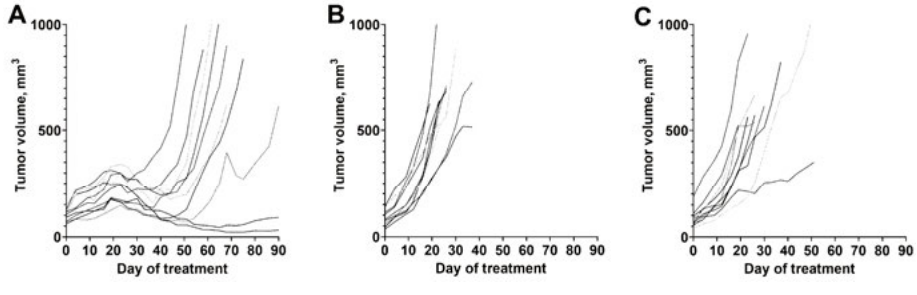

Figure 7. The growth of individual tumors in mice treated with (**A**) [^{188}Re]Re-$Z_{HER2:41071}$ (three times with 5 μg, 16 MBq), (**B**) non-labeled $Z_{HER2:41071}$ (three times with 5 μg), and (**C**) vehicle.

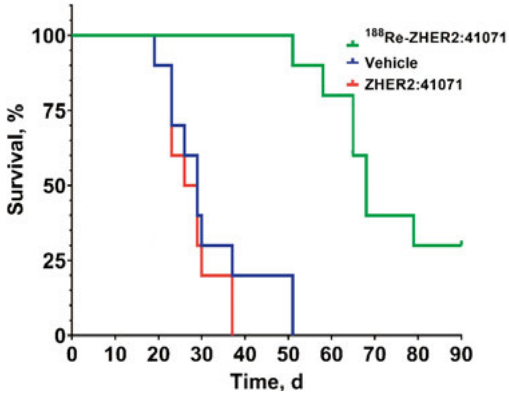

Figure 8. The survival of mice treated with [^{188}Re]Re-$Z_{HER2:41071}$, non-labeled $Z_{HER2:41071}$, and vehicle.

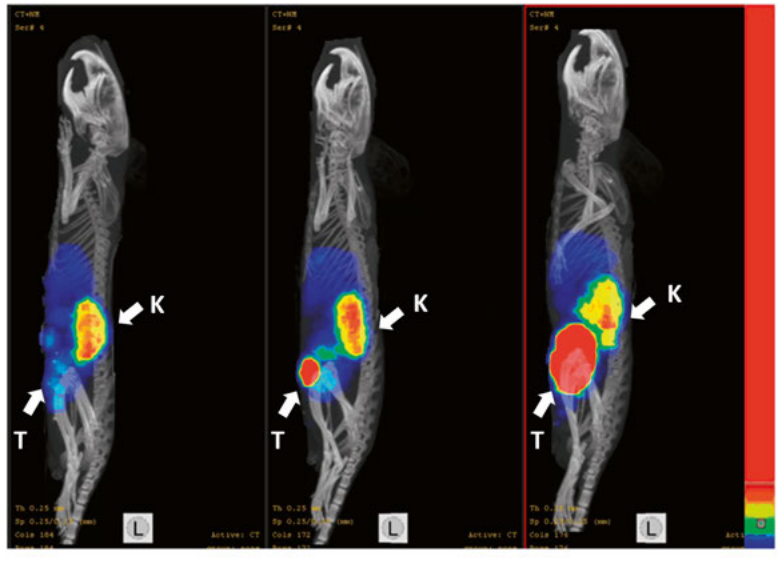

Figure 9. The SPECT-CT imaging using [^{99m}Tc]Tc-$Z_{HER2:41071}$ of mice with different tumor sizes after treatment with [^{188}Re]Re-ZHER2:41071 at day 35 after first injection. The scale is linear showing arbitrary units normalized to a count rate in kidneys. The arrows with the letter "T" point to the tumors, and the arrows with the letter "K" point to the kidneys.

Discussion and Conclusion

The anti-HER2 Affibody molecule, ZHER2:V2, with C-terminal -GGGC chelator, labeled with ^{99m}Tc [59] or ^{188}Re [53] has demonstrated excellent tumor targeting as well as low activity accumulation in kidneys. The second-generation of Affibody molecule, $Z_{HER2:41071}$, was produced with better stability and

lower immunogenic potential. Radiolabeled $Z_{HER2:41071}$ with ^{99m}Tc was evaluated and demonstrated similar targeting properties and biodistribution as [^{99m}Tc]Tc-ZHER2:V2, while [^{188}Re]Re-$Z_{HER2:41071}$ has not been evaluated so far.

This study showed that $Z_{HER2:41071}$ can be efficiently labeled with ^{188}Re, providing sufficient radiochemical yield and purity for clinical translation. Binding of [^{188}Re]Re-$Z_{HER2:41071}$ to HER2-expressing SKOV3 and SKBR3 cells was clearly HER2-mediated. Cellular processing evaluation of [^{188}Re]Re-$Z_{HER2:41071}$ showed its lower cellular retention compared with a counterpart containing a residualizing label, [^{188}Re]Re-ZHER2:2395, suggesting a non-residualizing property. In the biodistribution study, a pre-saturation of Na/I symporters by cold iodide was needed to reduce the uptake of metabolites of [^{188}Re]Re-$Z_{HER2:41071}$ in the salivary gland. In vivo biodistribution of [^{188}Re]Re-$Z_{HER2:41071}$ revealed rapid clearance of activity from all organs, including the kidney, which is important to enable delivery of sufficient absorbed dose to the tumor without exceeding the dose limitation to normal organs. Three injections of 16 MBq of [^{188}Re]Re-$Z_{HER2:41071}$ provided a significant delay of tumor growth, with a median survival of 68 days, compared with treatment with vehicle, 29 days, and with non-labeled $Z_{HER2:41071}$, 27.5 days. The injected dose was well-tolerated by treated animals, since no abnormal behavior and severe loss of body weight was observed and histopathology examination did not reveal any pathological changes in the liver and kidneys.

In conclusion, the experimental radionuclide therapy using [^{188}Re]Re-$Z_{HER2:41071}$ enabled the enhancement of survival of mice bearing human tumors without toxicity to the critical organ, the kidney.

Paper II Comparative Preclinical Evaluation of HER2-Targeting ABD-Fused Affibody® Molecules ^{177}Lu-ABY-271 and ^{177}Lu-ABY-027: Impact of DOTA Position on ABD Domain

Background and Aim

As mentioned earlier, fusion of the Affibody molecule with ABD is one of the potential ways to reduce the renal uptake. In further studies, a targeting agent, $Z_{HER2:2891}$-ABD-C-DOTA, denoted as ABY-027, has been developed based on the second generation of Affibody scaffold [35]. The versatile chelator DOTA, conjugated at the C-terminus of ABD, enabled site-specific labelling with a short-range beta emitter, lutetium-177. In the animal studies, [^{177}Lu]Lu-ABY-027 demonstrated a further reduction of renal and hepatic uptake compared with the first generation conjugate, [^{177}Lu]Lu-CHX-A"-DTPA-ABD-$(Z_{HER2:342})_2$. Meanwhile, a high tumor uptake of [^{177}Lu]Lu-ABY-027 has remained.

It was demonstrated that the biodistribution of radiolabeled Affibody molecules can be affected by the label position [61, 62]. It was also reported that helix one of ABD is not involved in the binding of ABD to albumin [63]. Therefore, we had the hypothesis that the position of a chelator on helix one, away from the albumin binding site, would reduce the interference of a chelate with albumin binding and decrease the renal uptake by stronger binding to albumin. To test the hypothesis, a cysteine was introduced at the position 76 of the $Z_{HER2:2891}$-ABD fusion and the DOTA chelator was conjugated to the cysteine for site-specific labeling (further denoted ABY-271) (Figure 10).

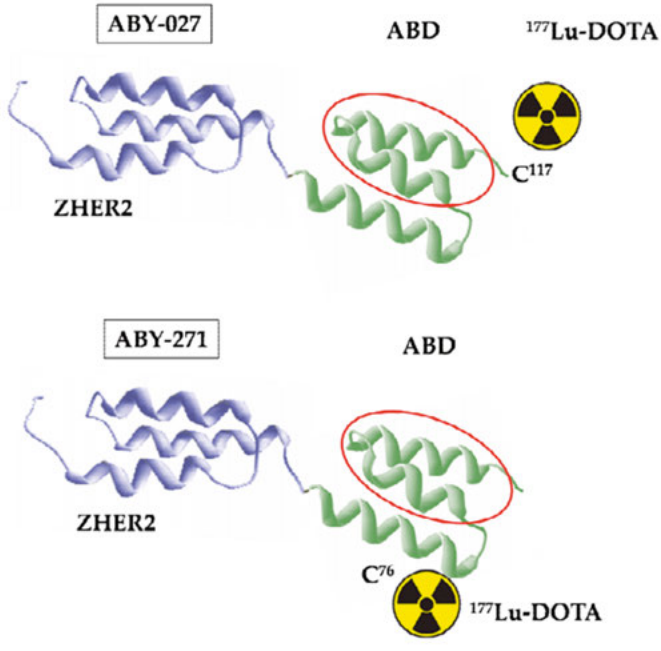

Figure 10. Structures of [^{177}Lu]Lu-ABY-271 and [^{177}Lu]Lu-ABY-027. The red line marks the segment of ABD where amino acids interacting with albumin are located.

ABY-271 was labeled with lutetium-177, and studied in vitro using HER2-expressing SKOV3 and BT474 cells, and in vivo in SKOV3 xenograft-bearing Balb/c nu/nu mice. Targeting properties and biodistribution of [^{177}Lu]Lu-ABY-271 were evaluated and compared with the properties of [^{177}Lu]Lu-ABY-027 in the same batch of xenograft-bearing mice. In order to evaluate the effect of fusion of $Z_{HER2:2891}$ with ABD, the biodistribution of [^{177}Lu]Lu-ABY-271 was compared with [^{177}Lu]Lu-ABY-025, which contained the same Affibody molecule and was conjugated to the same DOTA chelator but without fusion with ABD.

Results

ABY-271, ABY-027 and ABY-025 were labeled with lutetium-177 and purified using NAP-5 size-exclusion columns if needed, to get labeled compounds with high radiochemical purity (over 95%). In vitro stability data suggested that the labeling of ABY-271 with lutetium-177 was stable both under the EDTA challenge and during the incubation with human serum. In vitro specificity assay demonstrated that the binding of ^{177}Lu-labeled ABY-271 and ABY-027 to HER2-expressing SKOV3 and BT474 cells was HER2-mediated both in the presence and absence of HSA (Figure 11). The K_D of binding of

radiolabeled compounds to SKOV3 cells was in the sub-nanomolar range in the presence and absence of HSA (Table 8). Cellular retention profile showed a similar pattern for both variants in the presence of HSA. Over 85% of cell-associated activity remained after 24 h of interrupted incubation, with slow internalization (26% in SKOV3 and 16% in BT474) (Figure 12).

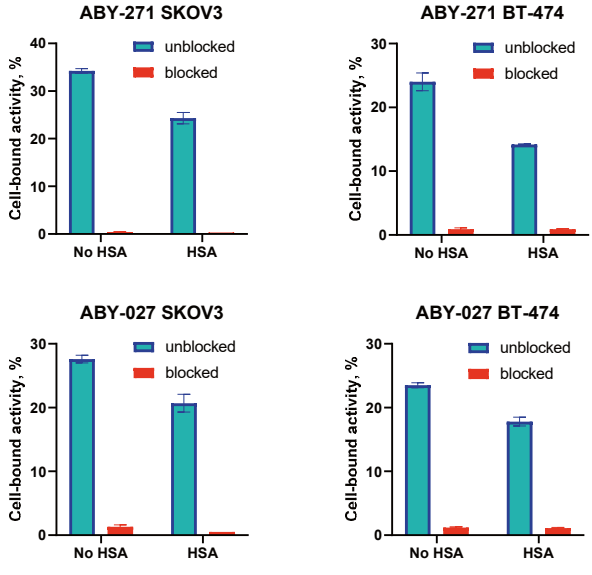

Figure 11. In vitro specificity test for ^{177}Lu-labeled ABY-271 and ABY-027 on SKOV3 and BT474 cells in absence and in the presence of HSA. The data are presented as an average value from 3 samples ± SD.

Table 8. InteractionMap evaluation of the affinity of ^{177}Lu-labeled ABY-271 and ABY-027 binding to HER2-expressing SKOV3 cells in the presence and absence of HSA.

	K_{D1} (pM)	K_{D2} (nM)	
[^{177}Lu]Lu-ABY-271 + HSA	321 ± 66	13.3 ± 2.9 (29-39%)	(n=5)
[^{177}Lu]Lu-ABY-271 no HSA	131 ± 31	24.3 ± 2.7 (10-12%)	(n=5)
[^{177}Lu]Lu-ABY-027 + HSA	674 ± 29	11.5 ± 0.7 (28%)	(n=2)
[^{177}Lu]Lu-ABY-027 no HSA	516 ± 47	17.0 ± 4.6 (15%)	(n=2)

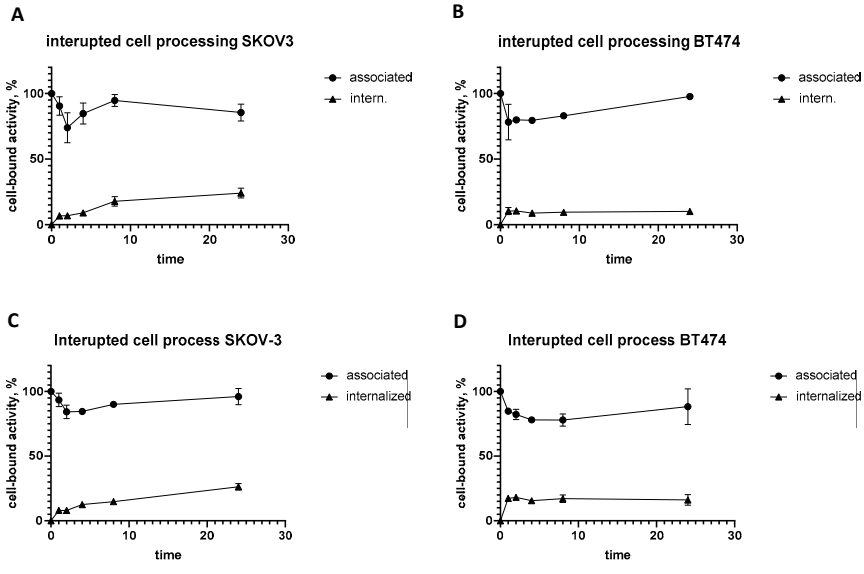

Figure 12. Cellular processing of [^{177}Lu]Lu-ABY-271 (**A**, **B**) and [^{177}Lu]Lu-ABY-027 (**C**, **D**) on SKOV3 and BT474 in the presence of HSA after interrupted incubation (average of 3 samples ± SD).

Tumor uptake of [^{177}Lu]Lu-ABY-271 in HER2-positive SKOV3 xenografts was significantly ($p < 0.0005$) higher than that in HER2-negative Ramos xenografts, which indicates specific binding of [^{177}Lu]Lu-ABY-271 in vivo (Figure 13). The uptake of [^{177}Lu]Lu-ABY-271 was 18-fold lower in kidney and 450-fold higher in blood compared with the uptake of [^{177}Lu]Lu-ABY-025 at 48 h after injection (Figure 14). Biodistribution of [^{177}Lu]Lu-ABY-271 in Balb/c nu/nu mice bearing SKOV3 xenografts demonstrated slow clearance from the blood, with a biological half-life of 28 h. The tumor uptake of [^{177}Lu]Lu-ABY-271 at 24 h p.i. was 18.2 ± 3.9 %ID/g, and was already higher than the uptake in blood and other organs and tissues.

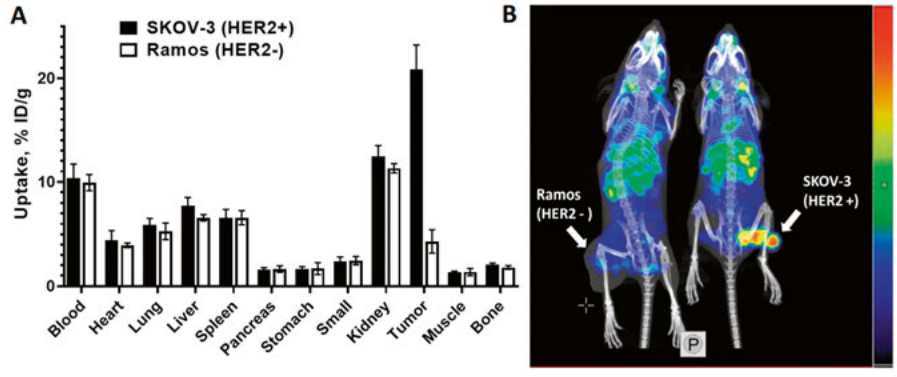

Figure 13. (**A**): In vivo binding specificity of [^{177}Lu]Lu-ABY-271 in Balb/c *nu/nu* mice bearing SKOV3 and Ramos xenografts at 48 h after injection. Results of ex vivo measurements are presented as %ID/g ± SD. (**B**): Imaging of [^{177}Lu]Lu-ABY-271 in Balb/c *nu/nu* mice bearing SKOV3 and Ramos xenografts at 48 h after injection.

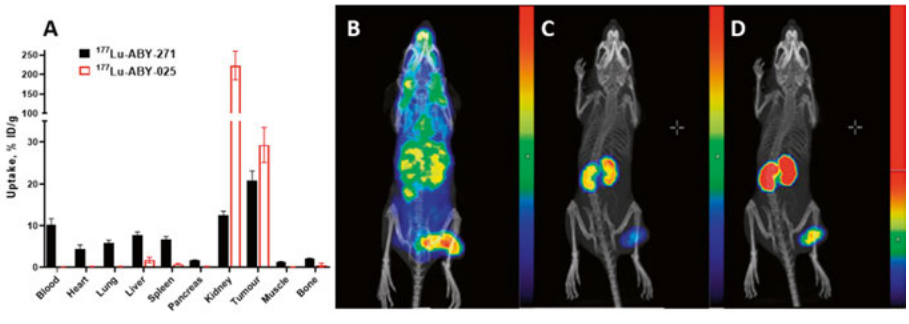

Figure 14. (**A**): Uptake of radioactivity at 48 h after injection of ^{177}Lu-labeled ABY-271 and ABY-025 in SKOV3 xenograft bearing mice (average of 4, %ID/g ± SD). (**B**): Imaging of distribution of [^{177}Lu]Lu-ABY-271. (**C**): Imaging of distribution of [^{177}Lu]Lu-ABY-025 (full scale). (**D**): Imaging of distribution of [^{177}Lu]Lu-ABY-025 (the scale is adjusted to the first red pixels in tumor).

The comparison of the biodistribution of ^{177}Lu-labeled ABY-271 and ABY-027 in HER2-expressing SKOV3 xenografts showed that tumor uptake of [^{177}Lu]Lu-ABY-027 was significantly higher ($p < 0.005$) than [^{177}Lu]Lu-ABY-271, while renal uptake of [^{177}Lu]Lu-ABY-027 was lower ($p < 0.0001$) than [^{177}Lu]Lu-ABY-271 at 48 h p.i.. The uptake of [^{177}Lu]Lu-ABY-027 in the kidney was significantly lower ($p < 0.0001$) than [^{177}Lu]Lu-ABY-271 at 168 h p.i., while tumor uptake of [^{177}Lu]Lu-ABY-027 and [^{177}Lu]Lu-ABY-271 were the similar (Figure 15).

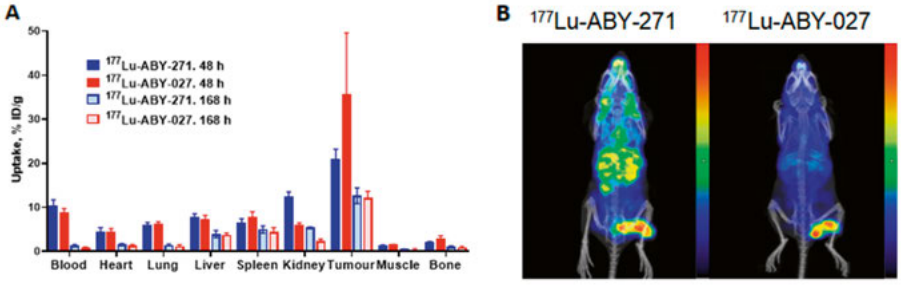

Figure 15. (**A**): The comparison of biodistribution of ^{177}Lu-labeled ABY-271 and ABY-027 in HER2-expressing SKOV3 xenograft-bearing Balb/c *nu/nu* mice at 48 and 168 h after injection. (**B**): Imaging of SKOV3 xenografts bearing mice injected with ^{177}Lu-labeled ABY-271 and ABY-027 at 48 h after injection.

Discussion and Conclusion

Affibody molecules can be considered as potential ligands for both targeted radionuclide imaging and therapy applications due to their small size, high specificity and affinity to the targeted receptors expressed on the cell membrane of malignant tumors. However, their high renal reabsorption limits the application of radiometal-labeled affibody molecules. One promising way to solve this problem is to fuse Affibody molecules to ABD, which binds to serum albumin in the circulation, in order to increase the size of the whole complex and extend the circulation time in the blood, aiming for reduction of the uptake in the kidney. In the previous study, an ABD fused Affibody molecule, ABY-027, labeled with lutetium-177, has demonstrated good properties of biodistribution in mice, suggesting that it is possibly appropriate for radionuclide therapy. In this study, a newly designed Affibody molecule fused to ABD, ABY-271, was developed, with a DOTA chelator conjugated on helix one of ABD. The aim of this study was to evaluate the targeting properties of [^{177}Lu]Lu-ABY-271 and compare them with [^{177}Lu]Lu-ABY-027 in the same batch of mice bearing HER2-positive xenografts.

Site-specific labeling of Affibody molecules with lutetium-177 created the feasibility to evaluate their in vitro and in vivo characteristics. The labeling and purification methods provided [^{177}Lu]Lu-ABY-271 with high radiochemical purity and high stability. Specific binding of both [^{177}Lu]Lu-ABY-271 and [^{177}Lu]Lu-ABY-027 to HER2-positive cells was confirmed in the presence and absence of HSA. LigandTracer measurements demonstrated binding to HER2-expressing cells with low nanomolar range affinity, which would be sufficient for in vivo targeting. Cellular retention profile showed a similar pattern in the presence of HSA for both variants. The major proportion of cell-

associated activity was membrane-bound, and a slow internalization was observed (less than 30% in 24 hours).

The results of the in vivo specificity test confirmed the new construct, [^{177}Lu]Lu-ABY-271, targeted HER2-positive SKOV3 xenografts specifically. Fusion of the Affibody molecule, $Z_{HER2:2891}$, with ABD increased its retention in the blood and its tumor-to-kidney ratio. This was demonstrated by the comparison of the biodistribution of [^{177}Lu]Lu-ABY-271 and [^{177}Lu]Lu-ABY-025 and confirmed by the imaging of biodistribution in mice model at 48 h p.i.. The biological half-life of ABY-271 was 28 h, which increased more than 50-fold compared to the half-life of 0.5 h of ABY-025 [64]. The uptake of [^{177}Lu]Lu-ABY-271 in the tumor exceeded uptake in any other organs at 24 h p.i. and afterwards. However, the tumor-to-kidney ratio of [^{177}Lu]Lu-ABY-271 was lower than three at any time point.

The comparison of the biodistribution of ^{177}Lu-labeled ABY-271 and ABY-027 showed that the tumor-to-kidney ratio of [^{177}Lu]Lu-ABY-271 was lower than that of [^{177}Lu]Lu-ABY-027. This suggests that [^{177}Lu]Lu-ABY-271 is less effective than [^{177}Lu]Lu-ABY-027 in delivering high-absorbed doses to tumors while minimizing high doses to the critical organ, the kidney. This comparison showed that the position of the DOTA chelator on ABD affected the biodistribution of ABD-fused Affibody molecules. In some previous studies, a similar positioning of a chelator on helix 3, further away from the binding site, was applied to Affibody molecules and showed non-affected affinity but a reduction of tumor uptake [62, 65]. One possible reason is that the placement of a chelator on helix one undermines the structural stability of the proteins in vivo. This results in rapider dissociation from albumin and reduced concentration in blood leading to lower tumor uptake.

To conclude, ^{177}Lu-labeled ABD-fused anti-HER2 Affibody molecule, ABY-271, specifically binds to HER2-expressing cells, and its targeting properties and biodistribution were suitable for radionuclide therapy. However, it is less effective than [^{177}Lu]Lu-ABY-027 for delivering high doses to tumors while avoiding high doses to kidneys. Even minor modifications in the molecular design of Affibody molecules, as small as positioning of DOTA chelator on the ABD, had a critical impact on the biodistribution properties. The positioning of the DOTA chelator at C-terminus of the anti-HER2 Affibody-ABD fusion protein is preferable compared to the position at 76 on the helix 1 of the albumin-binding moiety.

.

Paper III Biologic Evaluation of a Heterodimeric HER2-Albumin Targeted Affibody Molecule Produced by Chemo-Enzymatic Peptide Synthesis

Background and Aim

Affibody molecules, with small size (molecular weight 6.5 kDa) and high specificity and high affinity to their targets, were considered suitable ligands for radionuclide imaging and therapy. They can be produced both recombinantly and by chemical synthesis [66]. An anti-HER2 Affibody molecule has demonstrated a capability to effectively target and localize metastatic lesions in patients with HER2-expressing breast cancer [24]. As mentioned earlier, fusion of Affibody molecules with ABD has been demonstrated reduced renal uptake, due to binding of the fusion protein to the albumin in the host's circulation. So far, ABD-fused Affibody molecules were produced recombinantly, because it would be a challenge to synthesize such a large polypeptide (> 100 aa). Chemo-Enzymatic Peptide Synthesis (CEPS) might be an option to synthesize small peptide fragments separately and then ligate them using an engineered protein ligase called Omniligase [67].

This study aimed to investigate the hypotheses that a heterodimeric complex, containing an Affibody molecule and ABD, could be successfully produced using CEPS and this heterodimer would maintain a strong affinity for both HER2 and albumin, exhibit prolonged circulation time, and demonstrate specific targeting of HER2-expressing xenografts in a murine model. To test the hypothesis, a construct denoted as PEP40233, was produced using CEPS based on an anti-HER2 Affibody molecule, $Z_{HER2:2891}$, with a DOTA chelator at the N-terminus and an ABD at the C-terminus. PEP40233 was radiolabeled with lutetium-177, and its targeting properties were evaluated both in vitro and in vivo. To assess the impact of fusion with ABD, the biodistribution of [^{177}Lu]Lu-PEP40233 was compared to that of [^{177}Lu]Lu-ABY-025, which contains the same Affibody molecule conjugated with DOTA chelator but without ABD.

Results

The labeling of PEP40233 with ^{177}Lu was rapid and efficient, providing a radiochemical yield of over 98% after 30 min. In vitro binding of [^{177}Lu]Lu-PEP40233 to SKOV3 and BxPC3, with HER2-expression at high and low levels, respectively, was significantly lower ($p < 0.05$) after saturating HER2 receptors, both in the presence and absence of HSA (Figure 16). The affinity of

binding [^{177}Lu]Lu-PEP40233 to SKOV3 in the presence of HSA was the in sub-nanomolar range.

Biodistribution of [^{177}Lu]Lu-PEP40233 in mice bearing SKOV3 xenografts with a high HER2-expression, showed that the highest uptake among normal organs was in the kidneys at 48 h p.i. and uptake in the tumor was 1.6-fold higher than in the kidneys. Significantly lower ($p < 0.05$) tumor uptake than renal uptake was observed in BxPC3 xenografts with low HER2-expression. Activity accumulated in SKOV3 xenografts was significantly higher ($p < 0.05$) than that in BxPC3 xenografts (Figure 17A). Biodistribution of [^{177}Lu]Lu-PEP40233 showed significantly lower (9.4-fold, $p < 5 \times 10^{-5}$) renal uptake compared with [^{177}Lu]Lu-ABY-025 in SKOV3 bearing xenografts. The retention of [^{177}Lu]Lu-PEP40233 in the blood was 265-fold higher than that of [^{177}Lu]Lu-ABY-025. However, no significant ($p > 0.05$) difference was observed between tumor uptake of ^{177}Lu-labeled PEP40233 and ABY-025 (Figure 17B). SPECT/CT imaging of [^{177}Lu]Lu-PEP40233 in a mouse bearing SKOV3 xenograft at 48 h p.i. was in agreement with the biodistribution data (Figure 18).

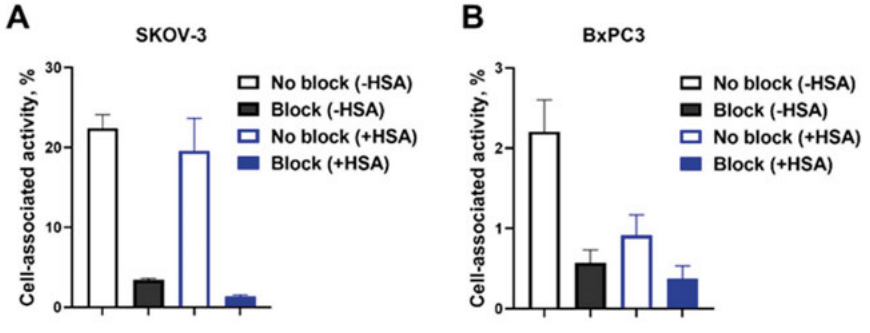

Figure 16. In vitro specificity of [^{177}Lu]Lu-PEP40233 binding to (**A**) SKOV-3 and (**B**) BxPC3 cells in the presence and absence of HSA. Block refers to pre-saturation of HER2 receptors with unlabeled PEP40233. The data are presented as an average value from 3 samples ± SD.

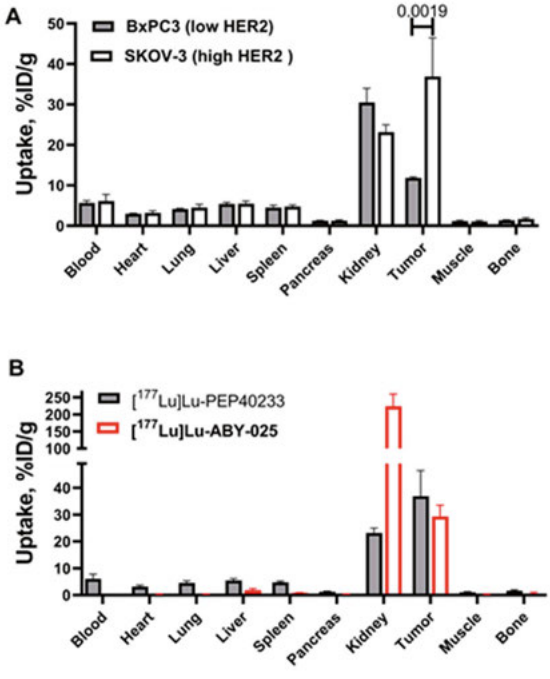

Figure 17. Biodistribution at 48 h p.i. (**A**) Biodistribution of [^{177}Lu]Lu-PEP40233 in Balb/c nu/nu mice bearing SKOV3 and BxPC3 xenografts. The data show higher accumulation in xenografts with higher HER2 expression. (**B**) Comparison of biodistribution of [^{177}Lu]Lu-PEP40233 and [^{177}Lu]Lu-ABY-025 in SKOV3 bearing xenografts. The data show clear reduction in the renal uptake and extension of residence in circulation for [^{177}Lu]Lu-PEP40233. Data are presented as an average value from four mice ± SD.

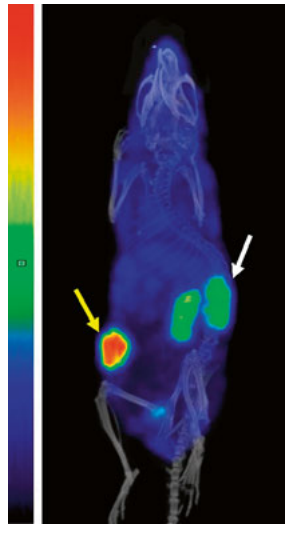

Figure 18. SPECT/CT imaging of mouse bearing SKOV3 xenograft 48 h p.i. of [^{177}Lu]Lu-PEP40233. Tumor (yellow arrow) and kidneys (white arrow) have elevated activity uptake, but tumor uptake exceeds the renal uptake. The scale is linear showing arbitrary units normalized to a maximum count rate.

Discussion and Conclusion

The use of peptide synthesis provides several benefits over recombinant production. These include precise control over the site-specific integration of prosthetic groups, the ability to incorporate unnatural amino acids to enhance resistance against proteases, and reduced cost for small-scale production. However, Affibody molecule together with ABD would be a long polypeptide (> 100 aa) and it is challenging to provide sufficient production yield. CEPS creates the possibility to synthesize such a long polypeptide by synthesizing shorter fragments separately and ligating them by an engineered protein ligase.

In this study, we evaluated the targeting properties of a CEPS-produced anti-HER2 Affibody molecule fused to ABD both in vitro and in vivo. The CEPS-produced PEP40233, labeled with a therapeutic radionuclide ^{177}Lu, demonstrated HER2-mediated specific binding and sub-nanomolar affinity to living cells expressing HER2, which is sufficient for a successful targeting of tumors [68]. Biodistribution of [^{177}Lu]Lu-PEP40233 showed significantly higher accumulation in SKOV3 xenografts than in BxPC3 xenografts at 48 h p.i.. This demonstrated that the tumor uptake of [^{177}Lu]Lu-PEP40233 was dependent on HER2 expression level, in other words, was HER2-specific in vivo. Retention of [^{177}Lu]Lu-PEP40233 in the blood was much longer compared with ABD-lacking [^{177}Lu]Lu-ABY-025, and the ligation with ABD reduced renal uptake 9.4-fold. Even though there was no significant difference

in tumor uptake, [^{177}Lu]Lu-PEP40233 has a higher tumor-to-kidney ratio than [^{177}Lu]Lu-ABY-025. However, the renal uptake of [^{177}Lu]Lu-PEP40233, 23.2 ± 1.8 %ID was much higher than the uptake of [^{177}Lu]Lu-ABY-027 (4.85 ± 0.2 %ID in Paper II) at 48 h, when the same tumor model, SKOV3 xenografts in nude mice was used [69]. This suggests the placement of DOTA chelator at the N-terminus of the construct was less ideal than that at the C-terminus.

To summarize, a CEPS-produced heterodimeric construct, containing an anti-HER2 Affibody molecule and ABD, demonstrated a high binding affinity to HER2 and albumin, a prolonged circulation time, reduced renal uptake, and specific and efficient targeting of HER2-positive xenografts in a murine model. Thus, the feasibility of fully synthetic production of long bi-specific Affibody construct using peptide synthesis was demonstrated. However, the placement of DOTA chelator at the N-terminus of the construct was suboptimal. This design results in a low tumor-to kidney ratio which is insufficient to be applied for TRT.

Paper IV Radionuclide Therapy of HER2-Expressing Xenografts Using [^{177}Lu]Lu-ABY-027 Affibody Molecule Alone and in Combination with Trastuzumab

Background and aims

Anti-HER2 Affibody molecule, ABY-027, containing ABD and C-terminus DOTA chelator, demonstrated HER2-specific binding and high tumor uptake when it was labeled with lutetium-177 [35]. It was suggested as a suitable candidate for radionuclide therapy. The attempt to further improve the molecular design by positioning DOTA chelator on the helix 1 of ABD or N-terminus resulted in suboptimal targeting properties [69, 70]. Therefore, ABY-027 which has the best tumor targeting properties was selected for experimental therapy study. It was demonstrated that HER2-expressing cancer cell lines are more sensitive to radiation when treated with trastuzumab [71], and clinically, the risk of locoregional recurrence was reduced in patients with breast cancer when receiving radiotherapy with adjuvant trastuzumab [72]. Structural studies showed that anti-HER2 Affibody molecules bind to HER2 on domain III and IV (Figure 19), which are far from the site where trastuzumab binds [73]. This enables us to combine Affibody-mediated radionuclide therapy and trastuzumab in the treatment of disseminated HER2-expressing cancers.

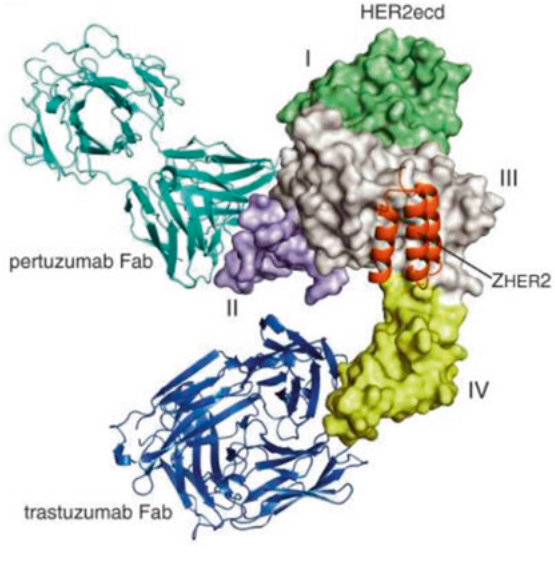

Figure 19. The epitope where anit-HER2 Affibody molecules bind to HER2 is far from trastuzumab epitope. (Reprinted from Eigenbrot, C et al. [73])

The goal of this study was to test the hypotheses that the targeted radionuclide therapy using [^{177}Lu]Lu-ABY-027 would prolong the survival of mice bearing

HER2-positive xenografts and that co-treatment with trastuzumab and [^{177}Lu]Lu-ABY-027 could prolong the survival even further. To test the hypotheses, in vitro studies were performed to evaluate if there is any interference of the binding of [^{177}Lu]Lu-ABY-027 and trastuzumab to HER2-expressing cells. The efficacy and efficiency of co-treatment of trastuzumab and radionuclide therapy using [^{177}Lu]Lu-ABY-027 was then evaluated and compared with mono-treatment using trastuzumab and [^{177}Lu]Lu-ABY-027 alone.

Results

In vitro binding affinity of [^{177}Lu]Lu-ABY-027 to living SKOV3 in the presence and absence of trastuzumab and/or HSA showed that adding trastuzumab reduced some interaction with high affinity but did not affect the lower-affinity interaction, while there was no interference with adding HSA (Table 9). Biodistribution results revealed that there was no significant difference in the uptake of [^{177}Lu]Lu-ABY-027 with or without pre-injection of trastuzumab in tumors and normal organs (Figure 20).

Table 9. Equilibrium dissociation constants (K_D) for interaction between [^{177}Lu]Lu-ABY-027 and HER2-expressing SKOV3 cells in the presence and absence of HSA and/or trastuzumab were analyzed by InteractionMap of LigandTracer Sensorgrams.

Parameter	K_{D1} (pM)	K_{D2} (nM)
[^{177}Lu]Lu-ABY-027 only	382.5 ± 53.0	15.7 ± 2.5
[^{177}Lu]Lu-ABY-027 with HSA	324.5 ± 75.7	16.5 ± 2.0
[^{177}Lu]Lu-ABY-027 with trastuzumab	502.5 ± 46.0	14.5 ± 0.1
[^{177}Lu]Lu-ABY-027 with trastuzumab and HSA	533.5 ± 43.1	14.2 ± 2.3

The pattern of tumor growth of mice in group treated with trastuzumab was similar to that treated with vehicle or unlabeled ABY-027, however some delay of the tumor growth was observed (Figure 21). Median survival of mice treated with trastuzumab was 55.5 days, which was significantly longer ($p < 0.05$) than that treated with vehicle (33 days) or unlabeled ABY-027 (42 days) (Figure 22). Tumor growth of mice in group treated with [^{177}Lu]Lu-ABY-027 or its combination with trastuzumab followed different patterns compared with patterns in the control groups (Figure 21). Significant reduction of mean tumor volume was observed in groups treated with [^{177}Lu]Lu-ABY-027 or its combination with trastuzumab from day 14 after treatment compared to that in the vehicle-treated group. Treatment with [^{177}Lu]Lu-ABY-027 alone significantly prolonged the median survival of mice to 77 days compared to

treatment with trastuzumab alone (Figure 22). Mice treated with the combination of trastuzumab and [^{177}Lu]Lu-ABY-027 did not reach median survival at the study termination (day 90), and there was no visible tumor in two animals in this group when the study was terminated. Therefore, the survival of mice in the combination group was significantly longer than that in the group treated with trastuzumab or [^{177}Lu]Lu-ABY-027 alone.

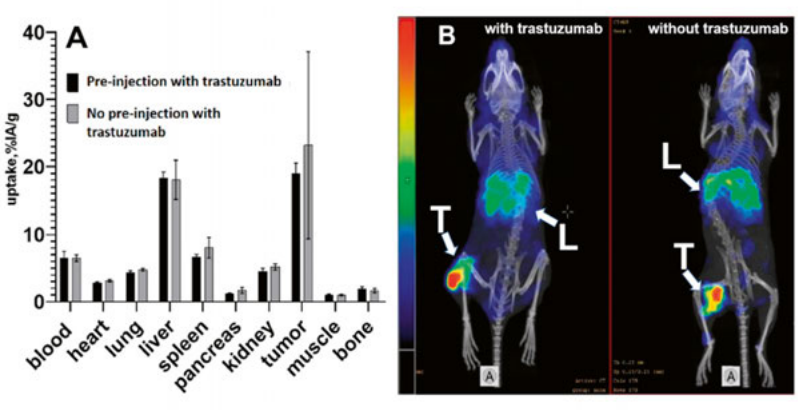

Figure 20. (A) Biodistribution of [^{177}Lu]Lu-ABY-027 with or without pre-injection of trastuzumab in HER2-expressing SKOV3 xenografts-bearing Balb/c nu/nu mice at 48 h p.i.. Uptake is expressed as %ID/g, which is corrected for decay and presented as average value from 4 mice ± SD. (B) Imaging of mice bearing SKOV-3 xenograft 48 h p.i. of [^{177}Lu]Lu-ABY-027 with or without pre-injection of trastuzumab using microSPECT/CT. Arrows point to tumors (T) and livers (L). The scale is linear showing arbitrary units normalized to a maximum count rate.

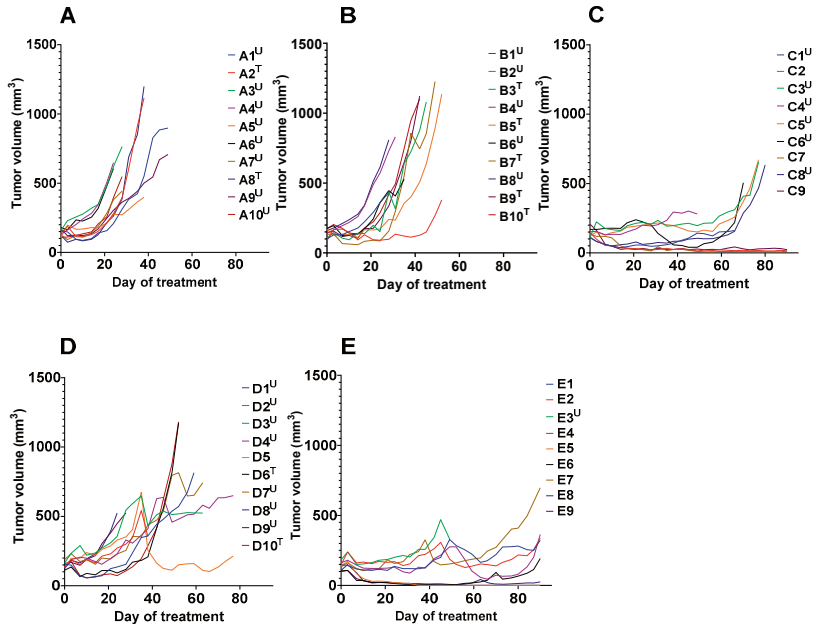

Figure 21. Tumor volume growth curves for individual mice from five groups receiving: (A) vehicle (1% BSA in PBS), (B) non-labeled ABY-027 (20 µg), (C) [^{177}Lu]Lu-ABY-027 (20 µg, 20 MBq), (D) trastuzumab, and (E) trastuzumab together with [^{177}Lu]Lu-ABY-027 (20 µg, 20 MBq). The doses and frequency of trastuzumab injections were 4 mg/kg for the first week and 2 mg/kg for the next five consecutive weeks. Mice were euthanized when xenograft volume exceeded 1000 mm^3 or bleeding ulcers were observed. Five groups of mice (10 animals per group) were used in the experiment.

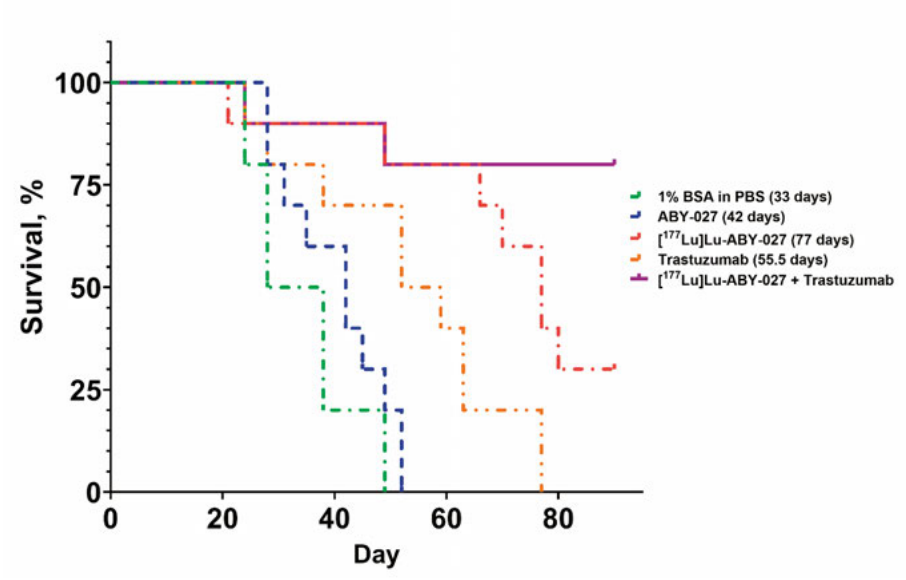

Figure 22. The survival of mice treated with vehicle (1% BSA in PBS), non-labeled ABY-027 (20 μg), [^{177}Lu]Lu-ABY-027 (20 μg, 20 MBq), trastuzumab, and combination of trastuzumab and [^{177}Lu]Lu-ABY-027 (20 μg, 20 MBq). The doses and frequency of trastuzumab injections were 4 mg/kg for the first week and 2 mg/kg for the next five consecutive weeks.

Discussion and Conclusion

Previous study demonstrated that fusion with ABD prolonged the retention time of the fused Affibody molecules in circulation due to their binding to albumin, and therefore reduced their renal uptake [34]. This approach was also proved to be useful for another scaffold protein, ADAPT6, in a preclinical study [74]. Another previous study suggested that the biodistribution of Affibody molecules could be affected by placement of chelator at different positions [65]. Many attempts of positioning of chelator at different sites have been evaluated based on the second generation of anti-HER2 Affibody molecule, ABY-027, to find out the optimal position in order to improve targeting properties [69, 70]. However, the molecular design of ABY-027 seems to be the most optimal for the moment.

To combine two targeted therapies simultaneously might be a potential approach to further enhance treatment outcomes. It would be attractive to combine radionuclide therapy with trastuzumab in the treatment of disseminated HER2-positive cancers. HER2-targeted Affibody molecules and trastuzumab bind to HER2 at different epitopes [73], which enables us to combine Affibody-based radionuclide therapy and trastuzumab treatment. A similar combination approach was used in a peptide nucleic acid (PNA)-based Affibody-

mediated pre-targeting system and demonstrated no interference with pretargeted delivery of Lu-177 to tumors when combined with trastuzumab in vivo [75]. The combination of radionuclide pre-targeting and trastuzumab therapy demonstrated greater efficacy than either of these treatments alone [75].

In this study, only a mild reduction of the affinity of an interaction of [^{177}Lu]Lu-ABY-027 with HER2-expressing SKOV3 cells was observed when adding trastuzumab. The reduced affinity was still in the sub-nanomolar range, which is sufficient for in vivo tumor targeting. Biodistribution of [^{177}Lu]Lu-ABY-027 at 48 h p.i. with or without pre-injection of trastuzumab indicated that the clinical dose of trastuzumab of 2 mg/kg should have no blocking effect for the binding of [^{177}Lu]Lu-ABY-027 to HER2-expressing SKOV3 xenografts. The experimental therapy demonstrated that the treatment of mice bearing HER2-expressing SKOV3 xenografts using [^{177}Lu]Lu-ABY-027 prolonged the median survival of animals to 77 days, compared to the mice treated with vehicle, 33 days. This effect was associated with specific delivery of Lu-177 to tumors and not with an anti-tumor effect of targeting agent, ABY-027 as such because the median survival of mice in the group treated with unlabeled ABY-027 was just 42 days, which was significantly shorter than that treated with [^{177}Lu]Lu-ABY-027. Mice treated with [^{177}Lu]Lu-ABY-027 have significantly longer median survival than those treated with a clinical dose of trastuzumab, which indicates that [^{177}Lu]Lu-ABY-027 provides a more efficient treatment than trastuzumab. A combination of [^{177}Lu]Lu-ABY-027 and trastuzumab demonstrated a better therapy outcome than either of those mono-treatments.

In conclusion, the use of [^{177}Lu]Lu-ABY-027 for radionuclide therapy demonstrated prolonged survival of mice bearing HER2-positive xenografts and it was shown to be more effective than treatment with trastuzumab alone. Moreover, the combination of [^{177}Lu]Lu-ABY-027 and trastuzumab further improved therapy outcomes and resulted in some tumor remissions. Importantly, all treatments were well-tolerated without kidney and liver toxicity. It would be promising to combine trastuzumab and radionuclide therapy using [^{177}Lu]Lu-ABY-027 for future clinical translation.

Paper V Evaluation of a novel ^{177}Lu-labelled therapeutic Affibody molecule with a deimmunized ABD domain and improved biodistribution profile

Background and Aim

We have previously demonstrated that [^{177}Lu]Lu-ABY-027, HER2-binding Affibody molecule, fused with an albumin-binding domain (ABD_{035}), provided HER2-specific targeting of human xenografts and a strong anti-tumor effect in a preclinical radionuclide therapy study [35, 76]. To facilitate clinical translation, a deimmunized ABD variant was developed and fused with an Affibody molecule, designated as PEP49989 (Figure 23).

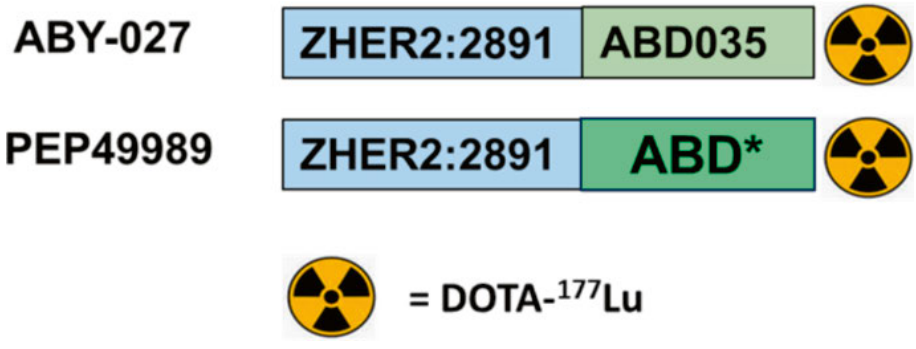

Figure 23. General architecture of tested constructs. ABD* refer to the deimmunized ABD variant [77].

The aim of the current study was to evaluate how this new ABD variant influences the targeting properties of Affibody molecule-based constructs for radionuclide therapy. For this purpose, targeting properties of [^{177}Lu]Lu-labelled PEP49989 and ABY-027 were compared directly. Since combination treatment is considered a promising approach for therapy of metastatic cancer, [^{177}Lu]Lu-PEP49989-mediated radionuclide therapy with and without trastuzumab was studied in tumor-bearing animals.

Results

The labeling of PEP49989 with lutetium-177 resulted in a yield of over 97% after 30 min incubation. The radiochemical purity of [^{177}Lu]Lu-PEP49989 was 99 ± 0% after 1 h incubation with a 500-fold molar excess of EDTA, which did not differ from the purity when incubated with PBS. In vitro binding of [^{177}Lu]Lu-PEP49989 to HER2-expressing SKOV3 and BT474 cells was significantly lower ($p < 0.001$) after saturation of HER2 receptors in blocked

groups, both in the presence and absence of HSA (Figure 24). The K_D of [^{177}Lu]Lu-PEP49989 binding to SKOV3 cells in the presence of HSA was 327 ± 12 pM, which was comparable to that of [^{177}Lu]Lu-ABY-027 (341 ± 4 pM). The cellular processing pattern was similar for both targeting agents. The binding was rapid during the first 2 h of incubation, the internalization in both cell lines was slow, less than 20% over 24 h.

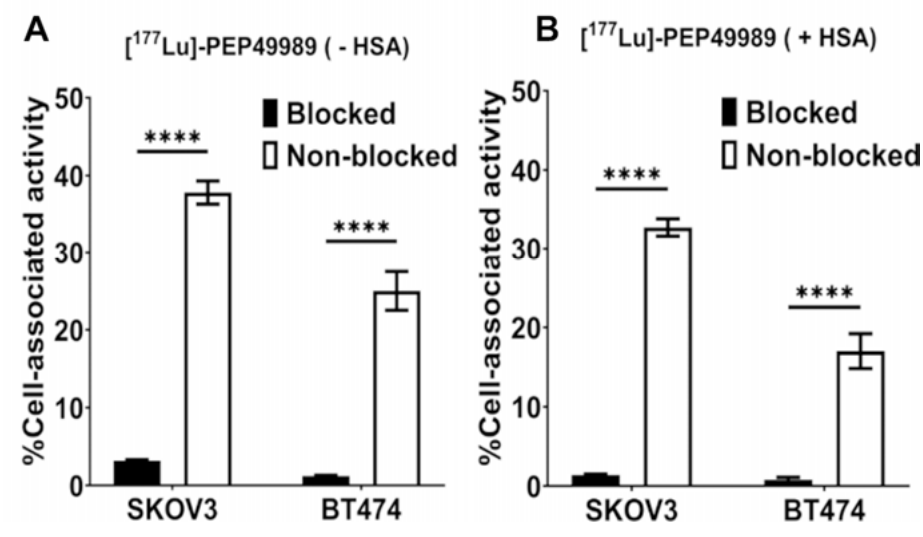

Figure 24. In vitro specificity of [^{177}Lu]Lu-PEP49989 binding to HER2-expressing SKOV3 and BT474 cells in the absence (A) and presence (B) of HSA. Blocked cells were treated with 1000-fold excess of an anti-HER2 Affibody conjugate. The data are presented as an average value from 3 samples ± SD. Asterisks (*) mark a highly significant difference ($p < 0.0005$, unpaired t-test).

In vivo specificity was evaluated by comparing of uptake of [^{177}Lu]Lu-PEP49989 in HER2-positive SKOV3 xenografts, HER2-negative Ramos xenografts. The uptake in Ramos xenografts was 9.5-fold lower than that in SKOV3 xenografts. With pre-injection of unlabeled PEP49989, the uptake was reduced significantly in SKOV3 xenografts (Figure 25 a). The results were confirmed by SPECT/CT imaging at 48 h p.i. in both SKOV3 and Ramos xenografts (Figure 25 b).

The biodistribution of [^{177}Lu]Lu-labelled ABY-027 and PEP49989 in mice bearing SKOV3 xenografts showed similar uptake of both constructs in the majority of organs. The renal uptake of [^{177}Lu]Lu-PEP49989 was 1.4-fold ($p < 0.05$) higher than the uptake of [^{177}Lu]Lu-ABY-027. However, the uptake of [^{177}Lu]Lu-PEP49989 in the liver was significantly ($p < 0.05$) lower, by 1.7-2.0 fold, than the uptake of [^{177}Lu]Lu-ABY-027. The tumor uptake of

[^{177}Lu]Lu-PEP49989 was significantly ($p < 0.05$, ca. 1.5-fold) higher than the uptake of [^{177}Lu]Lu-ABY-027 at 264 h p.i. (Figure 26).

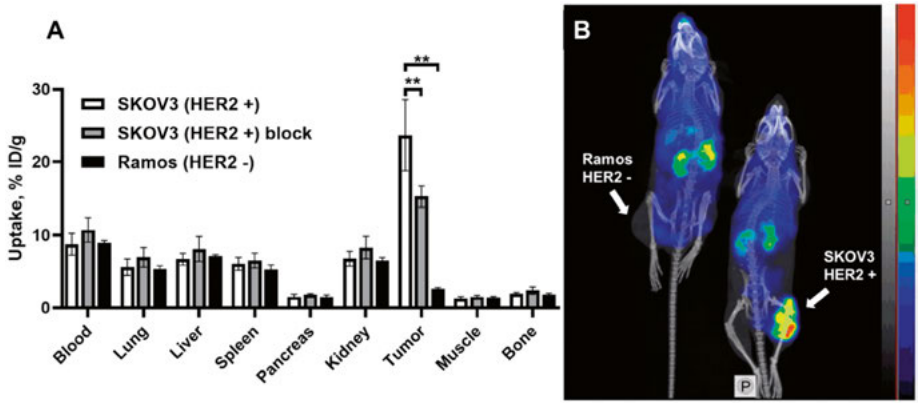

Figure 25. The HER2-specificity of [^{177}Lu]Lu-PEP49989 accumulation in tumours. (A) Biodistribution in mice HER2-positive SKOV3 and HER2-negative Ramos xenografts. In the blocking group, HER2 in SKOV3 xenografts were saturated by pre-injection of 700 µg unlabelled PEP49989. Asterisks (**) mark a highly significant difference ($p < 0.005$, unpaired t-test). Results are presented as % ID/g ± SD ($n = 4$–8). (B) Imaging of [^{177}Lu]Lu-PEP49989 in Balb/c nu/nu mice bearing SKOV3 and Ramos xenografts 48 h p.i.. The scale is linear showing arbitrary units normalized to a maximum count rate

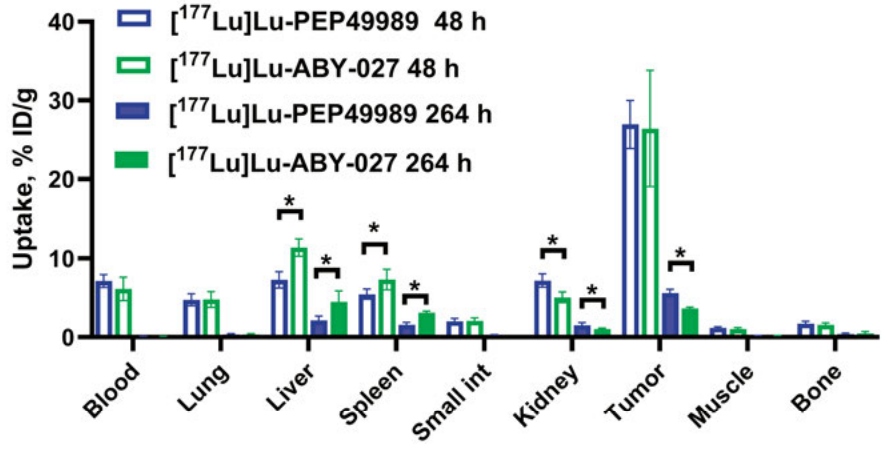

Figure 26. Biodistribution of [^{177}Lu]Lu-PEP49989 and [^{177}Lu]Lu-ABY-027 in tumor-bearing mice. Data are presented as an average ($n = 4$) value ± SD. Asterisks (*) mark a significant difference ($p < 0.05$, unpaired t-test).

Biodistribution of [^{177}Lu]Lu-PEP49989 in mice bearing SKOV3 xenografts at 4, 24, 48, 72, 168, 336 h p.i. showed a slow clearance from blood with a biological half-life of 23 h. By 24 h, the tumor uptake was higher than the uptake in normal organs. At 48 and 72 h p.i., the tumor uptake was 4-fold higher than the uptake in the kidney (Figure 27). Based on the biodistribution data, absorbed doses in mice were calculated, and the injected activity, 21 MBq, was selected for the experimental therapy study.

The median survival of mice treated with trastuzumab was 45 days, which was significantly longer than that of vehicle-treated mice (38 days). The median survival of mice treated with a single injection of [^{177}Lu]Lu-PEP49989 or a combination with trastuzumab was not reached at the end of experiment, and the survival time in these groups was significantly longer than that treated with trastuzumab alone (Figure 28). By the time of termination (day 90), complete tumor remission was achieved in five mice receiving combination therapy and in one of seven mice treated with a single injection of [^{177}Lu]Lu-PEP49989. No significant weight loss was observed in any group, except for mice treated with double injection of [^{177}Lu]Lu-PEP49989. Five out of seven mice that received a double injection experienced weight loss and had to be euthanized.

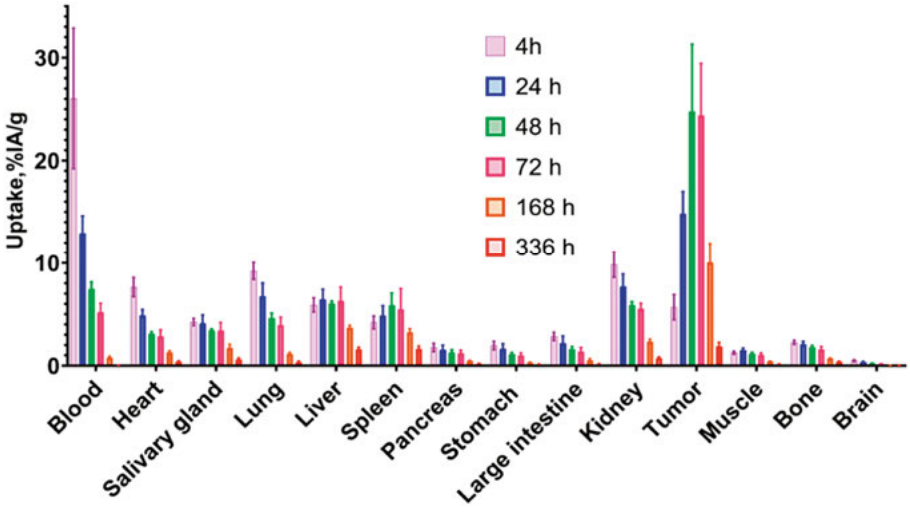

Figure 27. Biodistribution of [^{177}Lu]Lu-PEP49989 in mice bearing SKOV3 xenografts. Data are presented as an average (n = 4) value ± SD.

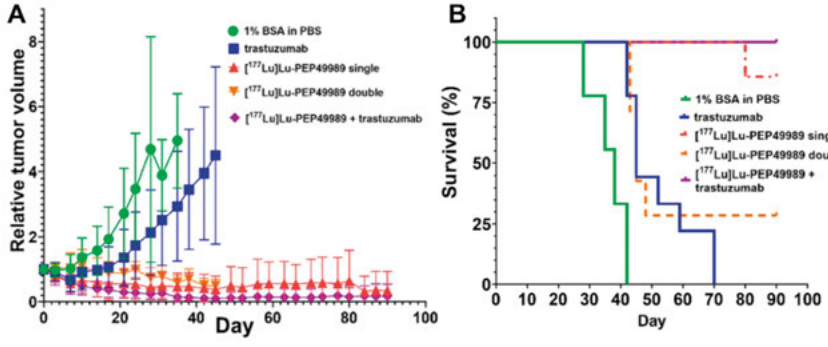

Figure 28. The therapeutic efficacy of [^{177}Lu]Lu-PEP49989 in comparison with trastuzumab, their combination and vehicle in mice bearing SKOV3 xenografts. (A) Tumor growth curves, (B) survival plot.

Discussion and Conclusion

We previously showed that [^{177}Lu]Lu-ABY-027 can significantly prolong the survival of mice bearing HER2-positive xenografts [76]. However, immunogenicity potential needs to be minimized for clinical translation. Therefore, T-cell epitopes were removed from ABD_{035} contained in ABY-027, generating a deimmunized ABD* variant. This domain was clinically evaluated in the Affibody-ABD fusion protein, izokibep, for treatment of psoriasis and showed no neutralizing antibodies or affected pharmacokinetics during three years of monthly treatment, indicating its safety [37, 78]. In this study, we investigated

the impact of this new ABD variant on the targeting properties and anti-tumor therapeutic effect of the ABD-fused Affibody molecule.

PEP49989 was successfully labeled with Lu-177 and demonstrated specific binding to HER2 in vitro (Figure 24) and in vivo (Figure 25). The affinity profile and cellular processing profile of [^{177}Lu]Lu-PEP49989 binding to living HER2-expressing cells were the same as the profiles of [^{177}Lu]Lu-ABY-027. Biodistribution in tumor-bearing mice showed comparable blood concentration of [^{177}Lu]Lu-PEP49989 to [^{177}Lu]Lu-ABY-027, while uptake of [^{177}Lu]Lu-PEP49989 in kidneys was slightly but significantly higher. This elevated renal uptake might be due to altered off-target interactions of the fusion protein resulting from the modification of the ABD moiety, since affinities of PEP49989 to both HSA and MSA (25 and 360 pM, respectively) were lower than affinities of ABY-027. Importantly, substitution of ABD_{035} with the deimmunized ABD* maintained targeting properties and reduced liver and spleen uptake, while enhancing tumor retention at later time points.

Therapeutic experiments showed that a single injection of [^{177}Lu]Lu-PEP49989 had better efficacy compared with trastuzumab. Pathology analysis identified bone marrow as the dose-limiting organ rather than kidney or liver toxicity. The efficacy of TRT can be enhanced by combination with other treatment approaches [79]. Clinical results show that trastuzumab increases the effect of external radiation therapy for patients with breast cancer [72, 80]. Our study showed that combination therapy with trastuzumab further increased complete remission rates. This combined approach was safer and more effective than repeated injections of TRT because of the different toxicity profiles of TRT and antibody-based therapy. Timing for the second injection might need to be optimized further to allow more time for recovery of the blood cells.

In conclusion, integration of the deimmunized albumin-binding domain had only a minor effect on the binding affinity of Affibody-based construct [^{177}Lu]Lu-PEP49989 to HER2-overexpressing cells. In mice, the new construct showed increased kidney uptake but reduced accumulation in liver and spleen compared with the parental ABD_{035}-containing [^{177}Lu]Lu-ABY-027, while maintaining blood retention and achieving higher tumor uptake at late time points. [^{177}Lu]Lu-PEP49989 demonstrated clear antitumor effects in experimental therapy, both as monotherapy and in combination with trastuzumab, highlighting its strong potential for clinical translation.

Concluding remarks

This thesis focused on the development and preclinical evaluation of HER2-targeted Affibody molecules for radionuclide therapy of HER2-overexpressing cancer. The overall goal of this thesis was to investigate different approaches to reduce the renal uptake of Affibody molecules in order to improve their tumor-targeting properties, biodistribution and the therapeutic efficacy in vivo, as well as the translational potential of these targeting agents.

In **Paper I**, a second-generation HER2-targeting Affibody molecule, [^{188}Re]Re-$Z_{HER2:41071}$, was evaluated for experimental therapy in HER2-expressing xenograft models. The study demonstrated reduced renal uptake when using this non-residualizing label, and a potent therapeutic effect and tumor regression with minimal toxicity.

Paper II compared two HER2-targeting Affibody-ABD fusion proteins labeled with ^{177}Lu, [^{177}Lu]Lu-ABY-271 and [^{177}Lu]Lu-ABY-027, differing in the position of the DOTA chelator on the ABD domain. This study revealed that the positioning of the chelator significantly affected the biodistribution and tumor uptake of the constructs. New construct [^{177}Lu]Lu-ABY-271 did not show an improvement in biodistribution profile and tumor-to-organ ratios, emphasizing the importance of rational molecular design for optimizing therapeutic agents.

In **Paper III**, a heterodimeric HER2-albumin-targeted Affibody molecule was generated using chemo-enzymatic peptide synthesis. This approach demonstrated that complex fusion proteins combining tumor-targeting and albumin-binding functionalities could be produced efficiently through semi-synthetic methods while retaining excellent binding properties and in vivo targeting. This study also showed the flexibility of the Affibody platform for modular engineering and cost-effective production.

Paper IV investigated the therapeutic efficacy of [^{177}Lu]Lu-ABY-027 alone and in combination with trastuzumab in mice bearing HER2-expressing xenografts. The combination therapy significantly enhanced tumor control and survival compared to monotherapy, without increasing toxicity. This finding highlighted the synergistic potential of combining TRT with antibody-based therapy, utilizing different mechanisms of HER2 targeting for improved clinical outcomes.

Finally, **Paper V** introduced a new construct, [^{177}Lu]Lu-PEP49989, in which a deimmunized ABD* replaced the original ABD_{035} to minimize potential immunogenicity. This new construct maintained high affinity for HER2 and albumin, showed improved biodistribution (lower liver and spleen uptake) and superior tumor retention compared to [^{177}Lu]Lu-ABY-027. It also provided remarkable therapeutic efficacy alone and in combination with trastuzumab. The results demonstrated that immunogenicity could be reduced without compromising targeting or therapeutic performance, representing an important step toward clinical translation.

Collectively, the results of this thesis demonstrate that HER2-targeting Affibody molecules represent a powerful and adaptable platform for targeted radionuclide therapy. By systematically improving molecular design, optimizing radionuclide labeling, and exploring synergistic therapeutic combinations, these studies have advanced the preclinical foundation for translating Affibody-based radiotherapeutics into the clinic.

Future Perspective

The work presented in this thesis demonstrates the potential of HER2-targeted Affibody molecules as highly-specific and versatile targeting agents for the development of radiotherapeutics for TRT. Through systematic optimization of molecular design, such as the position of DOTA chelators, introduction of deimmunized albumin-binding domains, and utilization of non-residualizing lable, these studies advance out knowledge about structure-property relationships and show the translational potential of Affibody-based therapeutics. Building further on these findings, several aspects can be considered for further exploration.

A key future direction is the clinical translation of the optimized construct [^{177}Lu]Lu-PEP49989, where safety, dosimetry, and therapeutic efficacy can be assessed in patients with HER2-positive malignancies. Currently, a Phase I clinical study (NCT07081555) of [^{177}Lu]Lu-PEP49989 is ongoing, and the first patient with HER2-positive metastatic breast cancer has been dosed on October 7, 2025 at Uppsala University Hospital in Sweden for the evaluation of safety, tolerability, and biodistribution.

Furthermore, combination of Affibody-based radionuclide therapy with clinically relevant monoclonal antibodies (e.g. pertuzumab), DNA damage repair inhibitors, or immune checkpoint blockade, represents promising strategies to enhance tumor control and minimize relapse.

From a radiochemistry standpoint, the exploration of alternative radionuclides such as terbium-161 (^{161}Tb) and actinium-225 (^{225}Ac) offers exciting opportunities. Their emission of conversion and Auger electrons or α-particles, respectively, could potentially improve treatment of micro-metastatic disease and heterogeneous tumors. The chemical robustness and refolding ability of Affibody scaffolds after heating make them well-suited for radiolabeling with these radionuclides.

In summary, Affibody molecules represent a flexible and powerful platform for the development of precise cancer therapies. The work presented in this thesis has shown that careful optimization of Affibody constructs can greatly improve their therapeutic performance and safety. Looking ahead, future research could focus on combining these optimized Affibody-based radiotherapeutics with other treatment strategies, to achieve stronger and more

durable anti-tumor effects. In addition, expanding their use beyond HER2 to other cancer-associated targets could further broaden their clinical value. Ultimately, these efforts aim to bring Affibody-based radionuclide therapy closer to routine clinical use, offering patients more effective and personalized treatment options.

Acknowledgments

I would like to express my deepest gratitude to all the people who have supported, encouraged, guided me throughout the journey of my PhD. This thesis would not have been possible without the contributions, kindness and love from many people.

First and foremost, my heartfelt gratitude goes to my supervisors, who have guided me with wisdom, kindness and endless patience.

Professor Vladimir Tolmachev, who introduced me to this research field already during my master's studies. Your inspiring lectures in radiochemistry sparked my interest and motivated me to join the group for my degree project. Thank you for believing in my potential and offering me this opportunity. As I started my PhD, we faced challenging moments together —residence permit struggles and the COVID pandemic —and I truly appreciate all the support and encouragement you gave me. Your mentorship for all the projects, presentations, and especially your attitude to science have meant a great deal to me.

Associate Professor Anzhelika Vorobyeva, who helped me a lot with many experiments during my PhD time, thank you for being such a great supervisor. I really appreciate your support especially in the last period of my PhD. All of the time and efforts you have spent on the preparation for my thesis and my defence.

Professor Anna Orlova, who is not one of my official supervisors, but is always available when I need help. I am grateful for your endless help in animal studies and many other things beyond research. Thank you for organization of Krägga meeting and arrangement with traveling for all international conferences. And a special thank you for being accompanying Tianqi when I was in ER during pandemic.

Professor Fredrik Frejd, who supported my research all the time during my PhD. Thank you for giving me a valuable perspective to research from the industry point of view, which greatly broadened my thinking. I always looked forward to the meeting with you and I really enjoyed our discussions. Your smile, energy and enthusiasm consistently encouraged me throughout my PhD.

Dr. Javad Garousi, my co-supervisor and good friend, thank you for your lectures in radiochemistry during my master. And thank you for sharing your valuable knowledge about biotechnology and all of other things.

Dr. Maryam Oroujeni, who guided me for the experiments even before my PhD. I joined you for my master degree project about PNA pre-targeting and learned so many things in the lab. Thank you for being patient when I had no idea about lab work.

I am grateful to be in a fantastic group that achieved success no matter how hard the situation was. **Ivan,** thank you for always being ready to help and sharing your knowledge and finding in spheroids and nanoparticles. **Eleftherios**, thank you for being sitting next to me and teaching me some Greek words, like Malaka and Enthusiastika. **Panagiotis**, thank you for sharing your knowledge in radiochemistry and for introducing me to your Greek friends during EANM conference. The handsome radiochemistry, **Athanasios**, thank you for the accompany for lunch and sharing drinks, coffee and also for the fun talks about cars and games. **Ekaterina** and **Karim** thank you for always being super nice and ready for help with many things. **Moeen** and **Enrique**, thank you for greetings every day and the fun talks all the time. **Ayman**, thank you for being always kind and sharing suggestions about half-time and defense. **Diaa**, thank you for all of the conversations about games and computers and your help with taking care of cells during my vacations. And to all of you, thank you so much for the fikas, fun talks, and being always back me up.

The work in this thesis, as well as many projects during my PhD, would never being successful without great collaborations. I would like to thank all collaborators in **Affibody AB**, **Erica, Olof, Caroline, Matilda, Elisabet Teresa,** and **Per**, who provided all of the Affibody molecules I mainly worked with. Thank you for providing such high-quality molecules and for all biotech related protein characterization. Special thank you to **Annika** and **Anna** who managed the process for the projects and arranged the meeting every month. I really enjoyed the meetings with you and appreciate your summary of every meeting.

And to another wonderful collaborator, **Mark**, thank you for your dosimetry calculations and recommendation of injected doses that ensured the success of the experimental therapies.

Olga Bragina, thank you for being part of my project and for sharing your valuable clinical insights.

To the warm-hearted people at PPP, thank you for providing such a great supportive platform. **Sergio, Veronika, Ola**, and **Ram**, who always help with providing nice environment for animals, always answer questions and resolve emergencies no matter how busy they are. Thank you for always being nice and for the help over the years. Thank you to **Olof, Bogdan, Mengfei, Hemantha, Hongchao, Amina, Francesco, Olivia, Jan, Pierre** and **Bo** for the fikas and talks.

To the big family at BMS, I am so grateful to be one of the members and share the great memories with you. Thank you, **Bo**, for always being kind and open for discussion, as well as for sharing the stories about running and your experiences for maintaining a house. Thank you, **Marika**, for sharing your knowledge about playing roles both in academic and company. In addition, I really appreciate that you kindly shared radionuclides which saved my studies for many times. Thank you, **Anja**, for being always open for discussion and sharing your tips about having a car and raising up a kid. Thank you, **Diana**, as well as **Christer**, for generously sharing your experiences —both scientific and personal, especially for those suggestions about electricity, house renovation, and so on. Thank you, **Olga** and **Hanna Yu**, for always keeping the labs and storage rooms in order and preparing things whatever is lacking. To **Torbjörn**, the Santa Claus of BMS, thank you for your lectures about detection techniques and dosimetry, your Christmas songs and all the time humorous talk. To **Hans**, thank you for your lectures about radiation during my master. To **Jörgen**, thank for the fun talks every year at Julbord.

And to all of the friends that I met at BMS, I am truly grateful for the time we spent together. Your kindness, encouragement and everyday support made my PhD journey lighter, warmer, and much more joyful.

To strong-and-independent-woman, **Tabassom**, thank you for being incredibly kind to both me and Mia. Thank you and **Sadra** for building her the slide and created unforgettable moments for us. Your hard work, positivity, and constant encouragement carried me through the entire PhD. I am deeply grateful.

To **Iris**, thank you for visiting and staying with us in the house. Thank you for playing with Mia, for the apple-picking, and for your cheerful greetings and encouragement. Your presence brought warmth and comfort.

To **Hanna**, **Amanda**, **Sara R** and **Saloni**, who are Mia's best friends, thank you for such wonderful companions in the lab and beyond. Thank you for the laughter we shared, the warm greetings in the corridor, and for celebrating good news.

To **Mehran**, you have encouraged me from the very beginning of my master studies. Thank you for the delicious food and the beautiful days spent together with **Ichi** and **Alma**. Your support always meant a lot to me.

To **Mahsa** and **Julieta**, thank you for your warm greetings and inspiring conversations. I wish you both the very best with your studies and future careers.

To **Preeti**, I truly enjoyed the time we spent together. Thank you for your friendship and for making those moments both fun and meaningful.

To all friends from Ridgeview, **Anna B**, **Guillermo**, **Sara L**, **Sina**, **Paolo**, **Piero**, **João**, thanks for sharing labs, instruments, and for happy Friday fikas. To **Jos**, thank you for sharing LigandTracer instruments and your knowledge about apple-juicing technique.

To **Yunqi** and **Maria**, thank you for joining me for the project and I wish you the best luck with your future.

To **Jinar**, **Sahar**, **Gillian**, **Amelia**, **Yufang**, **Amol**, **Nils**, **Sergey**, **Jessica**, **Enrica**, **Pengwei**, **Xi Lu**, **Marit**, **Nadja**, **Alice** and **many friends at Rudbeck**, thank you for warm greetings, smiles, fikas, and inspiring conversations.

To **Di Yu**, **Minglu**, **Yangyang**, thank you for accompanying every Thursday morning for the Swedish course, as well as for sharing life in our limited Swedish words, and talking freely during pause in Chinese.

To **Jielu**, thank you for your warm greetings, constant encouragement and all of the fun conversations we shared at PPP. To **Yongxiao** and **Rundong**, thank you for the food, the drinks, the card games and all the happy monments we spent together. To **Jichao**, **Zhongkai**, **Xuhui**, thank you for your friendship and staying connected across half the planet. Our video chats—despite the time zone differences—always made me feel supported and close to home.

To my family, I owe everything to your unwavering support.

To my **grandparents**, who spent the most time with me when I was little, thank you for your endless love and kindness.

To my **parents**, thank you for giving me life and supporting me on every step of this journey. No matter how surprising or uncertain my decisions my have seemed, you always encouraged me to move forward.

To my **mother-in-law**, thank you for embracing me with trust and understanding from the very beginning. You have traveled across half the globe to

visit us many times, especially after Mia's birth, you came to Sweden to help us through some of our most challenging and joyful moments. I deeply appreciate everything you have done for us.

To **Helen**, **Pierre**, **Lillie**, **Per**, and **Britt**, thank you for your kindness, warmth, and generous support. You drove several hours from Hallsberg to Uppsala on many occasions to visit us and offer help when we needed it most. Every time we visited you, we were welcomed with warm hospitality and good food. I am really grateful.

To **all my other family members**, although mountains and seas separate us, your love has always stayed close. Thank you for your love and concern.

To my wife, **Tianqi**, who was my desk mate, officemate, and my partner in every sense, thank you for all you dedication over the years. Your exceptional planning and organization have supported me both at work and in life. I could not have completed this journey without you.

To my daughter **Mia**, who was born during my PhD, you brought endless joy and meaning into my life. I wish you to grow up healthy, happy, confident, and outstanding.

Finally, my heartfelt gratitude goes to everyone who has cared for me, loved me, supported me, accompanied me, and helped me along the way. I would not be where I am today without you.

References

1. Bray, F., Laversanne, M., Sung, H., Ferlay, J., Siegel, R.L., Soerjomataram, I., Jemal, A. (2024) Global Cancer Statistics 2022: GLOBOCAN Estimates of Incidence and Mortality Worldwide for 36 Cancers in 185 Countries. *CA: A Cancer Journal for Clinicians*, 74(3):229–263.
2. Hanahan, D., Weinberg, R.A. (2011) Hallmarks of Cancer: The Next Generation. *Cell*, 144(5):646–674.
3. Zafar, A., Khatoon, S., Khan, M.J., Abu, J., Naeem, A. (2025) Advancements and limitations in traditional anti-cancer therapies: a comprehensive review of surgery, chemotherapy, radiation therapy, and hormonal therapy. *Discover Oncology*, 16(1):607.
4. Chabner, B., Roberts, T. (2005) Chemotherapy and the War on Cancer. *Nature Reviews Cancer*, 5:65–72.
5. Min, H.Y., Lee, H.Y. (2022) Molecular Targeted Therapy for Anticancer Treatment. *Experimental & Molecular Medicine*, 54:1670–1694.
6. Boumahdi, S., de Sauvage, F.J. (2020) The Great Escape: Tumour Cell Plasticity in Resistance to Targeted Therapy. *Nature Reviews Drug Discovery*, 19:39–56.
7. Sharma, P., Allison, J. P. (2015) The Future of Immune Checkpoint Therapy. *Science*, 348:56–61.
8. Gill, M.R., Falzone, N., Du, Y., Vallis, K.A. (2017) Targeted Radionuclide Therapy in Combined-Modality Regimens. *Lancet Oncology*, 18(7):e414–e423.
9. Herrmann, K., Schwaiger, M., Lewis, J.S., Solomon, S.B., McNeil, B.J., Baumann, M., Gambhir, S.S., Hricak, H., Weissleder, R. (2020) Radiotheranostics: A Roadmap for Future Development. *Lancet Oncology*, 21(3):e146–e156.
10. Yarden, Y., Pines, G. (2012) The ERBB network: at last, cancer therapy meets systems biology. *Nature Reviews Cancer*, 12(8):553-563.
11. Press, M.F., Cordon-Cardo, C., Slamon, D.J. (1990) Expression of the HER-2/neu Proto-Oncogene in Normal Human Adult and Fetal Tissues. *Oncogene*, 5(7):953–962.
12. Iqbal, N., Iqbal, N. (2014) Human Epidermal Growth Factor Receptor 2 (HER2) in Cancers: Overexpression and Therapeutic Implications. *Molecular Biology International*, 2014:852748.
13. Slamon, D.J., Clark, G.M., Wong, S.G., Levin, W.J., Ullrich, A., McGuire, W.L. (1987) Human Breast Cancer: Correlation of Relapse and Survival with Amplification of the HER-2/neu Oncogene. *Science*, 235(4785):177–182.
14. Perry, C.M., Wiseman, L.R. (1999) Trastuzumab. *BioDrugs*, 12(2):129–135.
15. Wu, X., Yang, H., Yu, X., Qin, J.J. (2022) Drug-resistant HER2-positive breast cancer: Molecular mechanisms and overcoming strategies. *Frontiers in Pharmacology*, 13:1012552.

16. Nord, K., Nilsson, J., Nilsson, B., Uhlén, M., Nygren, P.Å. (1995) A Combinatorial Library of an Alpha-Helical Bacterial Receptor Domain. *Protein Engineering*, 8(6):601–608.
17. Ståhl, S., Gräslund, T., Eriksson Karlström, A., Frejd, F.Y., Nygren, P.Å., Löfblom, J. (2017) Affibody Molecules in Biotechnological and Medical Applications. *Trends in Biotechnology*, 35(8):691–712.
18. Orlova, A., Magnusson, M., Eriksson, T. L., Nilsson, M., Larsson, B., Höidén-Guthenberg, I., Widström, C., Carlsson, J., Tolmachev, V., Ståhl, S., Nilsson, F. Y. (2006) Tumor Imaging Using a Picomolar Affinity HER2 Binding Affibody Molecule. *Cancer Research*, 66(8):4339–4348.
19. Mitran, B., Güler, R., Roche, F.P., Lindström, E., Selvaraju, R.K., Fleetwood, F., Rinne, S.S., Claesson-Welsh, L., Tolmachev, V., Ståhl, S., Orlova, A., Löfblom, J. (2018) Radionuclide Imaging of VEGFR2 in Glioma Vasculature Using Biparatopic Affibody Conjugate: Proof-of-Principle in a Murine Model. *Theranostics*, 8(16):4462–4476.
20. Malm, M., Kronqvist, N., Lindberg, H., Gudmundsdotter, L., Bass, T., Frejd, F.Y., Höidén-Guthenberg, I., Varasteh, Z., Orlova, A., Tolmachev, V., Ståhl, S., Löfblom, J. (2013) Inhibiting HER3-Mediated Tumor Cell Growth with Affibody Molecules Engineered to Low Picomolar Affinity by Position-Directed Error-Prone PCR-Like Diversification. *PLoS One*, 8(5):e62791.
21. Strand, J., Varasteh, Z., Eriksson, O., Abrahmsen, L., Orlova, A., Tolmachev, V. (2014) Gallium-68-Labeled Affibody Molecule for PET Imaging of PDGFRβ Expression In Vivo. *Molecular Pharmaceutics*, 11(11):3957–3964.
22. Oroujeni, M., Xu, T., Gagnon, K., Rinne, S.S., Weis, J., Garousi, J., Andersson, K.G., Löfblom, J., Orlova, A., Tolmachev, V. (2021) The Use of a Non-Conventional Long-Lived Gallium Radioisotope ^{66}Ga Improves Imaging Contrast of EGFR Expression in Malignant Tumours Using DFO-ZEGFR:2377 Affibody Molecule. *Pharmaceutics*, 13(2):292.
23. Sörensen, J., Sandberg, D., Sandström, M., Wennborg, A., Feldwisch, J., Tolmachev, V., Åström, G., Lubberink, M., Garske-Román, U., Carlsson, J., Lindman, H. (2014) First-in-Human Molecular Imaging of HER2 Expression in Breast Cancer Metastases Using the ^{111}In-ABY-025 Affibody Molecule. *Journal of Nuclear Medicine*, 55(5):730–735.
24. Sörensen, J., Velikyan, I., Sandberg, D., Wennborg, A., Feldwisch, J., Tolmachev, V., Orlova, A., Sandström, M., Lubberink, M., Olofsson, H., Carlsson, J., Lindman, H. (2016) Measuring HER2 Receptor Expression in Metastatic Breast Cancer Using [^{68}Ga]ABY-025 Affibody PET/CT. *Theranostics*, 6:262–271.
25. Fortin, M.A., Orlova, A., Malmström, P.U., Tolmachev, V. (2007) Labelling Chemistry and Characterization of [^{90}Y/^{177}Lu]-DOTA-ZHER2:342-3 Affibody Molecule, a Candidate Agent for Locoregional Treatment of Urinary Bladder Carcinoma. *International Journal of Molecular Medicine*, 19:285–291.
26. Garousi, J., Vorobyeva, A., Altai, M. (2020) Influence of Several Compounds and Drugs on the Renal Uptake of Radiolabeled Affibody Molecules. *Molecules*, 25:2673.
27. Altai, M., Membreno, R., Cook, B., Tolmachev, V., Zeglis, B.M. (2017) Pretargeted Imaging and Therapy. *Journal of Nuclear Medicine*, 58(10):1553–1559.
28. Westerlund, K., Altai, M., Mitran, B., Konijnenberg, M., Oroujeni, M., Atterbt, C., de Jong, M., Orlova, A., Mattsson, J., Micke, P., Karlström, A.E., Tolmachev, V. (2018) Radionuclide therapy of HER2-expressing human xenografts using an affibody molecule-based PNA-mediated pretargeting: In vivo proof-of-principle. *Journal of Nuclear Medicine*, 59:1092–1098.

29. Wållberg, H., Orlova, A. (2008) Slow internalization of anti-HER2 synthetic affibody monomer ^{111}In-DOTA-ZHER2:342-pep2: Implications for development of labeled tracers. *Cancer Biotherapy and Radiopharmaceuticals*, 23:435–442.
30. Tolmachev, V., Mume, E., Sjöberg, S., Frejd, F.Y., Orlova, A. (2009) Influence of valency and labelling chemistry on in vivo targeting using radioiodinated HER2-binding Affibody molecules. *European Journal of Nuclear Medicine and Molecular Imaging*, 36(4):692-701.
31. Oroujeni, M., Rinne, S.S., Vorobyeva, A., Loftenius, A., Feldwisch, J., Jonasson, P., Chernov, V., Orlova, A., Frejd, F.Y., Tolmachev, V. (2021) Preclinical Evaluation of ^{99m}Tc-ZHER2:41071, a Second-Generation Affibody-Based HER2-Visualizing Imaging Probe with a Low Renal Uptake. *International Journal of Molecular Sciences*, 22:2770.
32. Jonsson, A., Dogan, J., Herne, N., Abrahmsén, L., Nygren, P.Å. (2008) Engineering of a Femtomolar Affinity Binding Protein to Human Serum Albumin. *Protein Engineering, Design & Selection*, 21(8):515–527.
33. Nilsen, J., Trabjerg, E., Grevys, A., Azevedo, C., Brennan, S.O., Stensland, M., Wilson, J., Sand, K.M.K., Bern, M., Dalhus, B., Roopenian, D.C., Sandlie, I., Rand, K.D., Andersen, J.T. (2020) An Intact C-Terminal End of Albumin Is Required for Its Long Half-Life in Humans. *Communications Biology*, 3(1):181.
34. Tolmachev, V., Orlova, A., Pehrson, R., Galli, J., Baastrup, B., Andersson, K., Sandström, M., Rosik, D., Carlsson, J., Lundqvist, H., Wennborg, A., Nilsson, F.Y. (2007) Radionuclide therapy of HER2-positive microxenografts using a ^{177}Lu-labeled HER2-specific Affibody molecule. *Cancer Research*, 67(6):2773-2782.
35. Orlova, A., Jonsson, A., Rosik, D., Lundqvist, H., Lindborg, M., Abrahmsén, L., Ekblad, C., Frejd, F.Y., Tolmachev, V. (2013) Site-Specific Radiometal Labeling and Improved Biodistribution Using ABY-027, a Novel HER2-Targeting Affibody Molecule-Albumin-Binding Domain Fusion Protein. *Journal of Nuclear Medicine*, 54(6):961–968.
36. Altai, M., Liu, H., Ding, H., Mitran, B., Edqvist, P.H., Tolmachev, V., Orlova, A., Gräslund, T. (2018) Affibody-Derived Drug Conjugates: Potent Cytotoxic Molecules for Treatment of HER2 Over-Expressing Tumors. *Journal of Controlled Release*, 288:84–95.
37. Gerdes, S., Staubach, P., Dirschka, T., Wetzel, D., Weirich, O., Niesmann, J., da Mota, R., Rothhaar, A., Ardabili, M., Vlasitz, G., Feldwisch, J., Osterling Koskinen, L., Ohlman, S., Peloso, P.M., Brun, N.C., Frejd, F.Y. (2023) Izokibep for the Treatment of Moderate-to-Severe Plaque Psoriasis: A Phase II, Randomized, Placebo-Controlled, Double-Blind, Dose-Finding Multicentre Study Including Long-Term Treatment. *British Journal of Dermatology*, 189(4):381–391.
38. Taylor, P.C., Mease, P.J., de Vlam, K., Mpofu, S., Wetzel, D., Stevens, A.M., Wiens, B., Koskinen, L.O., Ohlman, S., Feldwisch, J., Frejd, F.Y., Brun, N.C., Brandt-Juergens, J., Drescher, E., Dokoupilova, E., Rowińska-Osuch, A., Abdel-Kader Martin, N., Behrens, F. (2025) Efficacy and safety of izokibep in patients with active psoriatic arthritis: a randomised, double-blind, placebo-controlled, phase 2 study. *Annals of the Rheumatic Diseases*, 2:S0003-4967(25)00815-5.
39. Sgouros, G., Bodei, L., McDevitt, M.R., Nedrow, J.R. (2020) Radiopharmaceutical therapy in cancer: clinical advances and challenges. *Nature Reviews Drug Discovery*, 19(9):589-608.

40. Primac, I., Tabury, K., Tasdogan, A., Baatout, S., Herrmann, K. (2025) The Molecular Blueprint of Targeted Radionuclide Therapy. *Nature Reviews Clinical Oncology*, 22(11):869–894.
41. Ghaseminejad, S., De Sarno, D., Bauman, G., Lee, T.Y. (2025) Framework to Calculate ^{225}Ac, ^{177}Lu, and ^{161}Tb Radiation Dose and Biological Effect in Metastatic Castration-Resistant Prostate Cancer Treatment. *Medical Physics*, 52(8):e18035.
42. Stokke, C., Kvassheim, M., Blakkisrud, J. (2022) Radionuclides for Targeted Therapy: Physical Properties. *Molecules*, 27(17):5429.
43. Palmedo, H., Guhlke, S., Beets, A.L., Sartor, J., Knapp, F.F., Bogatzky, J., Biersack, H.J. (1997) Rhenium-188-HEDP for Pain Palliation of Bone Metastases: First Clinical Results. *European Journal of Nuclear Medicine*, 24:962.
44. Bunjes, D., Buchmann, I., Duncker, C., Seitz, U., Kotzerke, J., Wiesneth, M., et al. (2001) Rhenium-188-Labeled Anti-CD66 (a, b, c, e) Monoclonal Antibody to Intensify the Conditioning Regimen Prior to Stem Cell Transplantation for Patients with High-Risk Acute Myeloid Leukemia or Myelodysplastic Syndrome: Results of a Phase I–II Study. *Blood*, 98:565–572.
45. Klein, M., Lotem, M., Peretz, T., Zwas, S.T., Mizrachi, S., Liberman, Y., et al. (2013) Safety and Efficacy of 188-Rhenium-Labeled Antibody to Melanin in Patients with Metastatic Melanoma. *Journal of Skin Cancer*, 2013:828329.
46. Kumar, A., Srivastava, D.N., Chau, T.T.M., Long, H.D., Bal, C., Chandra, P., et al. (2007) Inoperable Hepatocellular Carcinoma: Transarterial ^{188}Re HDD-Labeled Iodized Oil for Treatment—Prospective Multicenter Clinical Trial. *Radiology*, 243:509–519.
47. Strosberg, J., El-Haddad, G., Wolin, E., Hendifar, A., Yao, J., Chasen, B., Mittra, E., Kunz, P.L., Kulke, M. H., Jacene, H., Bushnell, D., O'Dorisio, T.M., Baum, R. P., Kulkarni, H.R., Caplin, M., Lebtahi, R., Hobday, T., Delpassand, E., Van Cutsem, E., Benson, A., Srirajaskanthan, R., Pavel, M., Mora, J., Berlin, J., Grande, E., Reed, N., Seregni, E., Öberg, K., Lopera Sierra, M., Santoro, P., Thevenet, T., Erion, J.L., Ruszniewski, P., Kwekkeboom, D., Krenning, E.; NETTER-1 Trial Investigators. (2017) Phase 3 Trial of ^{177}Lu-Dotatate for Midgut Neuroendocrine Tumors. *New England Journal of Medicine*, 376(2):125–135.
48. Morris, M.J., Castellano, D., Herrmann, K., de Bono, J.S., Shore, N.D., Chi, K.N., Crosby, M., Piulats, J.M., Fléchon, A., Wei, X.X., Mahammedi, H., Roubaud, G., Študentová, H., Nagarajah, J., Mellado, B., Montesa-Pino, Á., Kpamegan, E., Ghebremariam, S., Kreisl, T.N., Wilke, C., Lehnhoff, K., Sartor, O., Fizazi, K.; PSMAfore Investigators. (2024) ^{177}Lu-PSMA-617 versus a Change of Androgen Receptor Pathway Inhibitor Therapy for Taxane-Naïve Patients with Progressive Metastatic Castration-Resistant Prostate Cancer (PSMAfore): A Phase 3, Randomised, Controlled Trial. *Lancet*, 404(10459):1227–1239.
49. Dadgar, H., Pashazadeh, A., Norouzbeigi, N., Assadi, M., Al-Balooshi, B., Baum, R.P., Al-Ibraheem, A., Haidar, M., Beheshti, M., Geramifar, P., Vali, R., Mohammadi, S., Dash, S., Malasani, V., Cimini, A., Ricci, M., Esmail, A.A., Murad, S., Marafi, F., Treglia, G., Khalaf, A.N., Anwar, F.M., Usmani, S., Omar, Y., Muhsin, H., Tyurin, I.E., Zakhary, A., Al-Sebaie, S., Cortes, D.M., AlHashim, M., Arabi, H., Zaidi, H. (2025) Targeted Radioligand Therapy: Physics and Biology, Internal Dosimetry and Other Practical Aspects During ^{177}Lu/^{225}Ac Treatment in Neuroendocrine Tumors and Metastatic Prostate Cancer. *Theranostics*, 15(10):4368–4397.

50. Pouget, J.P., Lozza, C., Deshayes, E., Boudousq, V., Navarro-Teulon, I. (2015) Introduction to Radiobiology of Targeted Radionuclide Therapy. *Frontiers in Medicine*, 2:12.
51. Pandit-Taskar, N., Iravani, A., Lee, D., Jacene, H., Pryma, D., Hope, T., Saboury, B., Capala, J., Wahl, R.L. (2021) Dosimetry in Clinical Radiopharmaceutical Therapy of Cancer: Practicality Versus Perfection in Current Practice. *Journal of Nuclear Medicine*, 62(Suppl 3):60S–72S.
52. Bodei, L., Michael Tuttle, R., Grewal, R.K., Mauguen, A., Augensen, F., Abusamra, M., Mahajan, S., Jayaprakasam, V.S., Osborne, J.R., Haque, S., Wong, B.Z.Y., Ghossein, R. A., Fagin, J., Schöder, H., Ho, A., Humm, J.L., Larson, S.M. (2024) Toward Individualized Dosimetry for Radiopharmaceutical Therapy in Day-to-Day Clinical Practice of Nuclear Oncology: Overcoming Heterogeneity of Radiation-Absorbed Dose to Tumor and Critical Organs. *European Journal of Nuclear Medicine and Molecular Imaging*, 51(2):325–329.
53. Altai, M., Wållberg, H., Honarvar, H., Strand, J., Orlova, A., Varasteh, Z., Sandström, M., Löfblom, J., Larsson, E., Strand, S. E., et al. (2014) ^{188}Re-ZHER2:V2, a Promising Affibody-Based Targeting Agent Against HER2-Expressing Tumors: Preclinical Assessment. *Journal of Nuclear Medicine*, 55:1842–1848.
54. Tolmachev, V., Tran, T.A., Rosik, D., Sjoberg, A., Abrahmsen, L., Orlova, A. (2012) Tumor targeting using affibody molecules: Interplay of affinity, target expression level, and binding site composition. *Journal of Nuclear Medicine*, 53:953–960.
55. Prang, N., Preithner, S., Brischwein, K., Göster, P., Wöppel, A., Müller, J., Steiger, C., Peters, M., Baeuerle, P.A., da Silva, A.J. (2005) Cellular and Complement-Dependent Cytotoxicity of Ep-CAM-Specific Monoclonal Antibody MT201 Against Breast Cancer Cell Lines. *British Journal of Cancer*, 92(2):342–349.
56. Larbouret, C., Gaborit, N., Chardès, T., Coelho, M., Campigna, E., Bascoul-Mollevi, C., Mach, J.P., Azria, D., Robert, B., Pélègrin, A. (2012) In Pancreatic Carcinoma, Dual EGFR/HER2 Targeting with Cetuximab/Trastuzumab Is More Effective Than Treatment with Trastuzumab/Erlotinib or Lapatinib Alone: Implication of Receptor Down-Regulation and Dimer Disruption. *Neoplasia*, 14:121–130.
57. DeFazio-Eli, L., Strommen, K., Dao-Pick, T., Parry, G., Goodman, L., Winslow, J. (2011) Quantitative Assays for the Measurement of HER1–HER2 Heterodimerization and Phosphorylation in Cell Lines and Breast Tumors: Applications for Diagnostics and Targeted Drug Mechanism of Action. *Breast Cancer Research*, 13(2):R44.
58. Rinne, S.S., Xu, T., Dahlsson Leitao, C., Ståhl, S., Löfblom, J., Orlova, A., Tolmachev, V., Vorobyeva, A. (2020) Influence of Residualizing Properties of the Radiolabel on Radionuclide Molecular Imaging of HER3 Using Affibody Molecules. *International Journal of Molecular Sciences*, 21(4):1312.
59. Wållberg, H., Orlova, A., Altai, M., Hosseinimehr, S.J., Widström, C., Malmberg, J., Ståhl, S., Tolmachev, V. (2011) Molecular design and optimization of ^{99m}Tc-labeled recombinant affibody molecules improves their biodistribution and imaging properties. *Journal of Nuclear Medicine*, 52:461–469.
60. Deutsch, E., Libson, K., Vanderheyden, J.L., Ketring, A.R., Maxon, H.R. (1986) The Chemistry of Rhenium and Technetium as Related to the Use of Isotopes of These Elements in Therapeutic and Diagnostic Nuclear Medicine. *International Journal of Radiation Applications and Instrumentation Part B: Nuclear Medicine and Biology*, 13:465–477.

61. Ekblad, T., Orlova, A., Feldwisch, J., Wennborg, A., Karlström, A. E., Tolmachev, V. (2009) Positioning of ^{99m}Tc-Chelators Influences Radiolabeling, Stability and Biodistribution of Affibody Molecules. *Bioorganic & Medicinal Chemistry Letters*, 19(14):3912–3914.
62. Perols, A., Honarvar, H., Strand, J., Selvaraju, R., Orlova, A., Karlström, A.E., Tolmachev, V. (2012) Influence of DOTA Chelator Position on Biodistribution and Targeting Properties of ^{111}In-Labeled Synthetic Anti-HER2 Affibody Molecules. *Bioconjugate Chemistry*, 23(8):1661–1670.
63. Johansson, M.U., Frick, I.M., Nilsson, H., Kraulis, P.J., Hober, S., Jonasson, P., Linhult, M., Nygren, P.Å., Uhlén, M., Björck, L., Drakenberg, T., Forsén, S., Wikström, M. (2002) Structure, Specificity, and Mode of Interaction for Bacterial Albumin-Binding Modules. *Journal of Biological Chemistry*, 277(10):8114–8120.
64. Ahlgren, S., Orlova, A., Wållberg, H., Hansson, M., Sandström, M., Lewsley, R., Wennborg, A., Abrahmsén, L., Tolmachev, V., Feldwisch, J. (2010) Targeting of HER2-Expressing Tumors Using ^{111}In-ABY-025, a Second-Generation Affibody Molecule with a Fundamentally Reengineered Scaffold. *Journal of Nuclear Medicine*, 51:1131–1138.
65. Honarvar, H., Strand, J., Perols, A., Orlova, A., Selvaraju, R.K., Eriksson Karlström, A., Tolmachev, V. (2014) Position for Site-Specific Attachment of a DOTA Chelator to Synthetic Affibody Molecules Has a Different Influence on the Targeting Properties of ^{68}Ga- Compared to 111In-Labeled Conjugates. *Molecular Imaging*, 13.
66. Löfblom, J., Feldwisch, J., Tolmachev, V., Carlsson, J., Ståhl, S., Frejd, F. Y. (2010) Affibody Molecules: Engineered Proteins for Therapeutic, Diagnostic and Biotechnological Applications. *FEBS Letters*, 584:2670–2680.
67. Toplak, A., Teixeira de Oliveira, E.F., Schmidt, M., Rozeboom, H.J., Wijma, H.J., Meekels, L.K.M., de Visser, R., Janssen, D.B., Nuijens, T. (2021) From thiol-subtilisin to omniligase: Design and structure of a broadly applicable peptide ligase. *Computational and Structural Biotechnology Journal*, 19:1277–1287.
68. Schmidt, M.M., Wittrup, K.D. (2009) A Modeling Analysis of the Effects of Molecular Size and Binding Affinity on Tumor Targeting. *Molecular Cancer Therapeutics*, 8:2861–2871.
69. Liu, Y., Vorobyeva, A., Xu, T., Orlova, A., Loftenius, A., Bengtsson, T., Jonasson, P., Tolmachev, V., Frejd, F.Y. (2021) Comparative Preclinical Evaluation of HER2-Targeting ABD-Fused Affibody® Molecules ^{177}Lu-ABY-271 and ^{177}Lu-ABY-027: Impact of DOTA Position on ABD Domain. *Pharmaceutics*, 13:839.
70. Liu, Y., Güler, R., Liao, Y., Vorobyeva, A., Widmark, O., Meuleman, T. J., Koijen, A., van den Bos, L. J., Naasz, R., Bodenko, V., Orlova, A., Ekblad, C., Tolmachev, V., Frejd, F. Y. (2022) Biologic Evaluation of a Heterodimeric HER2-Albumin Targeted Affibody Molecule Produced by Chemo-Enzymatic Peptide Synthesis. *Pharmaceutics*, 14(11):2519.
71. Liang, K., Lu, Y., Jin, W., Ang, K.K., Milas, L., Fan, Z. (2003) Sensitization of Breast Cancer Cells to Radiation by Trastuzumab. *Molecular Cancer Therapeutics*, 2(11):1113–1120.
72. Kiess, A.P., McArthur, H.L., Mahoney, K., Patil, S., Morris, P.G., Ho, A., Hudis, C.A., McCormick, B. (2012) Adjuvant Trastuzumab Reduces Locoregional Recurrence in Women Who Receive Breast-Conservation Therapy for Lymph Node-Negative, Human Epidermal Growth Factor Receptor 2-Positive Breast Cancer. *Cancer*, 118:1982–1988.

73. Eigenbrot, C., Ultsch, M., Dubnovitsky, A., Abrahmsén, L., Härd, T. (2010) Structural Basis for High-Affinity HER2 Receptor Binding by an Engineered Protein. *Proceedings of the National Academy of Sciences of the United States of America*, 107:15039–15044.
74. Garousi, J., von Witting, E., Borin, J., Vorobyeva, A., Altai, M., Vorontsova, O., Konijnenberg, M.W., Oroujeni, M., Orlova, A., Tolmachev, V., Hober, S. (2021) Radionuclide therapy using ABD-fused ADAPT scaffold protein: Proof of principle. *Biomaterials*, 266:120381.
75. Oroujeni, M., Tano, H., Vorobyeva, A., Liu, Y., Vorontsova, O., Xu, T., Westerlund, K., Orlova, A., Tolmachev, V., Karlström, A. E. (2022) Affibody-Mediated PNA-Based Pretargeted Cotreatment Improves Survival of Trastuzumab-Treated Mice Bearing HER2-Expressing Xenografts. *Journal of Nuclear Medicine*, 63:1046–1051.
76. Liu, Y., Xu, T., Vorobyeva, A., Loftenius, A., Bodenko, V., Orlova, A., Frejd, F. Y., Tolmachev, V. (2023) Radionuclide Therapy of HER2-Expressing Xenografts Using [^{177}Lu]Lu-ABY-027 Affibody Molecule Alone and in Combination with Trastuzumab. *Cancers*, 15(9):2409.
77. Zurdo, J., Arnell, A., Obrezanova, O., Smith, N., Gómez de la Cuesta, R., Gallagher, T.R., Michael, R., Stallwood, Y., Ekblad, C., Abrahmsén, L., Höidén-Guthenberg, I. (2015) Early implementation of QbD in biopharmaceutical development: a practical example. *BioMed Research International*, 2015:605427.
78. Klint, S., Feldwisch, J., Gudmundsdotter, L., Dillner Bergstedt, K., Gunneriussón, E., Höidén Guthenberg, I., Wennborg, A., Nyborg, A. C., Kamboj, A.P., Peloso, P.M., Bejker, D., Frejd, F.Y. (2023) Izokibep: Preclinical Development and First-in-Human Study of a Novel IL-17A Neutralizing Affibody Molecule in Patients with Plaque Psoriasis. *mAbs*, 15:2209920.
79. Bodei, L., Herrmann, K., Schöder, H., Scott, A. M., Lewis, J.S. (2022) Radiotheranostics in Oncology: Current Challenges and Emerging Opportunities. *Nature Reviews Clinical Oncology*, 19:534–550.
80. Peterson, D.J., Truong, P.T., Sadek, B.T., Alexander, C.S., Wiksyk, B., Shenouda, M., Raad, R.A., Taghian, A.G. (2014) Locoregional recurrence and survival outcomes by type of local therapy and trastuzumab use among women with node-negative, HER2-positive breast cancer. *Annals of Surgical Oncology*, 21(11):3490–3496.

Acta Universitatis Upsaliensis

Digital Comprehensive Summaries of Uppsala Dissertations from the Faculty of Medicine 2224

Editor: The Dean of the Faculty of Medicine

A doctoral dissertation from the Faculty of Medicine, Uppsala University, is usually a summary of a number of papers. A few copies of the complete dissertation are kept at major Swedish research libraries, while the summary alone is distributed internationally through the series Digital Comprehensive Summaries of Uppsala Dissertations from the Faculty of Medicine. (Prior to January, 2005, the series was published under the title "Comprehensive Summaries of Uppsala Dissertations from the Faculty of Medicine".)

Distribution: publications.uu.se
urn:nbn:se:uu:diva-572728

ACTA UNIVERSITATIS
UPSALIENSIS
2026